Fale uderzeniowe i przyspieszanie cząstek w gromadach galaktyk

Jacek Niemiec

Instytut Fizyki Jądrowej PAN, Kraków

Współpracownicy:
Oleh Kobzar - Obserwatorium Astronomiczne UJ, Kraków
Stella Boula - Instytut Fizyki Jądrowej PAN, Kraków
Takanobu Amano, Masahiro Hoshino - University of Tokyo, Japan
Karol Fułat - University of Potsdam, Germany
Shuichi Matsukiyo - Kyushu University, Japan
Yosuke Matsumoto - Chiba University, Japan
Martin Pohl - Desy-Zeuthen/University of Potsdam, Germany

Seminarium Astrofizyczne Instytutu Fizyki UJ, 5 czerwca 2024 r.

Galaxy clusters

- clusters of galaxies and filaments that connect them are the largest structures in the Universe
- they form through a hierarchical sequence of mergers and accretion of smaller systems
- galaxy mergers dissipate huge amounts of gravitational energy (~10^{64} ergs) mainly at shocks, and this energy is channeled into heating of the gas in the intra-cluster-medium (ICM), large-scale ICM motion, and also into non-thermal particles and magnetic fields
- merging galaxy clusters show radio synchrotron emission from relativistic electrons in the form of:
  - giant radio halos in the center of galaxy clusters - emission originates from electrons accelerated through scattering off MHD turbulence and/or secondary electrons resulting from cosmic-ray proton interactions with ICM
  - giant radio relics at cluster outskirts - associated with Mpc-scale shocks that accelerate electrons

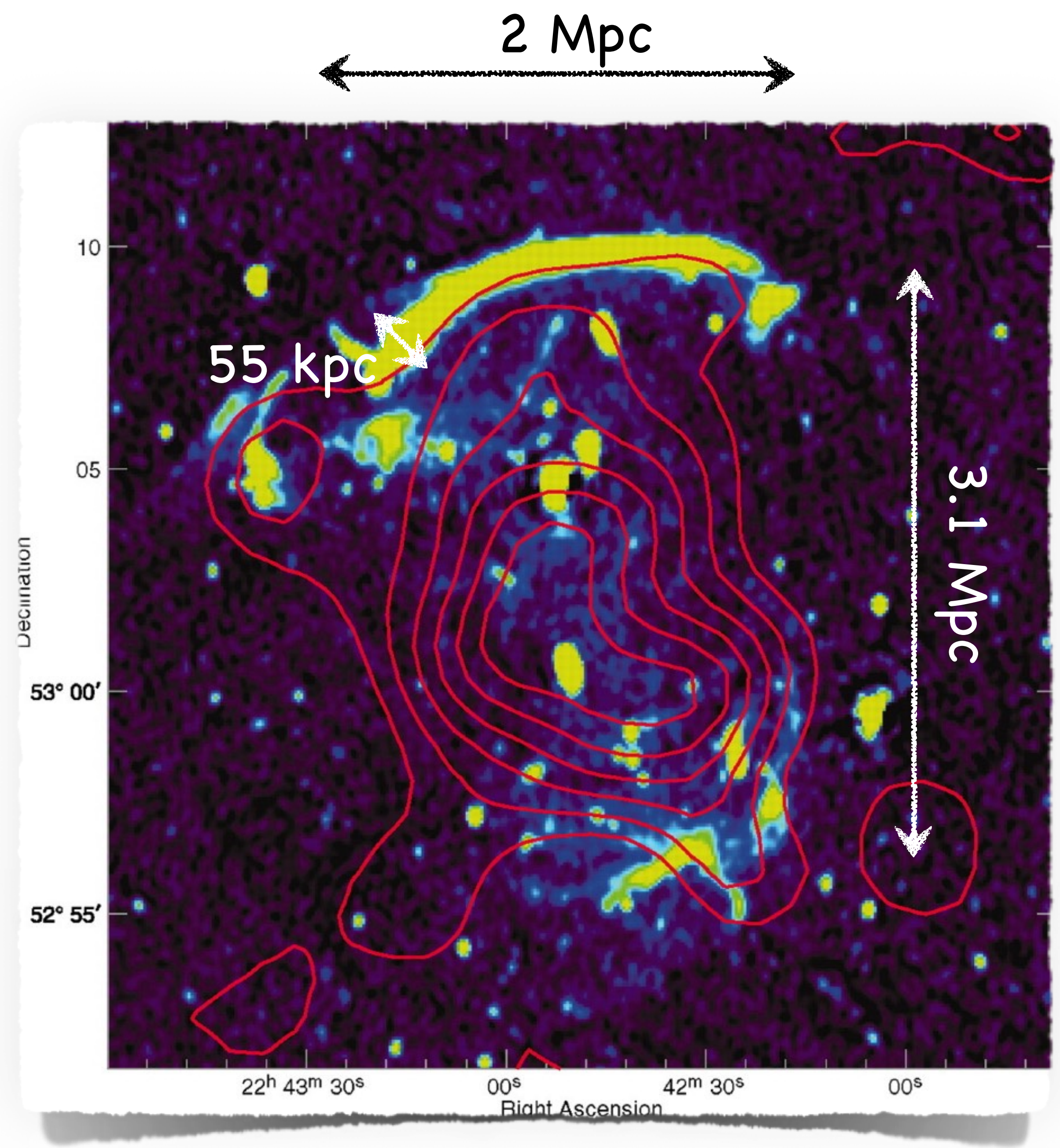

CIZA J2242.8+5301 (Sausage)
WSRT radio image at 1.4 GHz
X-ray emission (ROSAT, red contours)
van Weeren et al. (2010)

Merger shocks

- X-ray observations of radio relics indicate that most energetic merger shocks have low Mach numbers ($M_s < 5$, $M_A < 10$); shock velocities $v_{sh} \sim 10^3$ km/s
- intracluster medium (ICM) is hot = high plasma beta ($\beta >> 1$)
  - T ~ 1-10 keV
  - B ~ 1 μG
  - n ~ 10^{-4}-10^{-5} cm^{-3}
- high-energy CR electrons assumed to be generated via Diffusive Shock Acceleration (DSA)

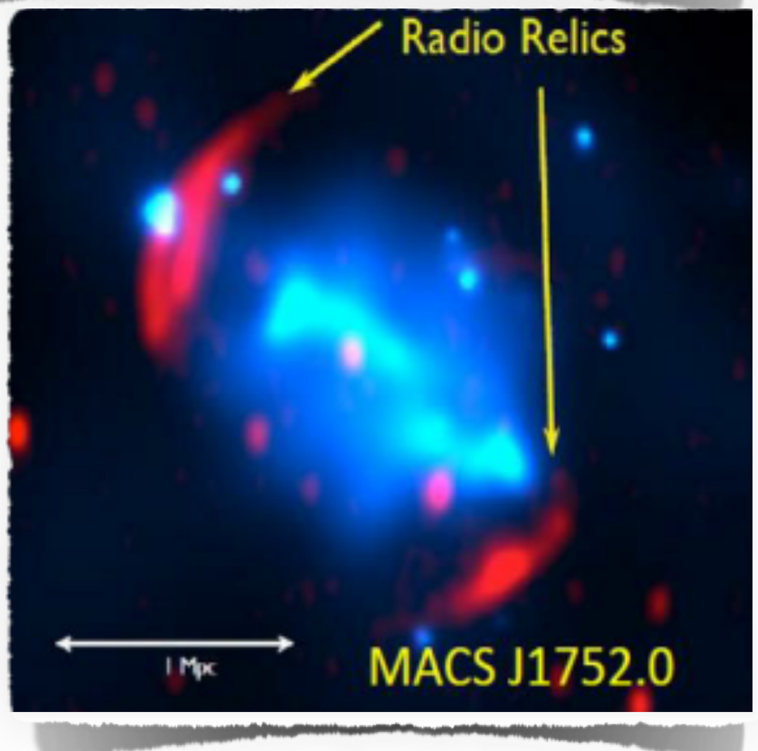

White - optical (Hubble)
Blue - X-ray (Chandra)
Red - radio (VLA)

Alfvenic Mach number: $M_A = \frac{v_{sh}}{v_A}$

Sonic Mach number: $M_s = \frac{v_{sh}}{c_s}$

Plasma beta: $\beta = p_{th}/p_{mag}$

$$v_A = \frac{B_0}{\sqrt{\mu_0(N_e m_e + N_i m_i)}}$$

$$c_s = \sqrt{2\Gamma k_B T_i / m_i}$$

DSA at merger shocks

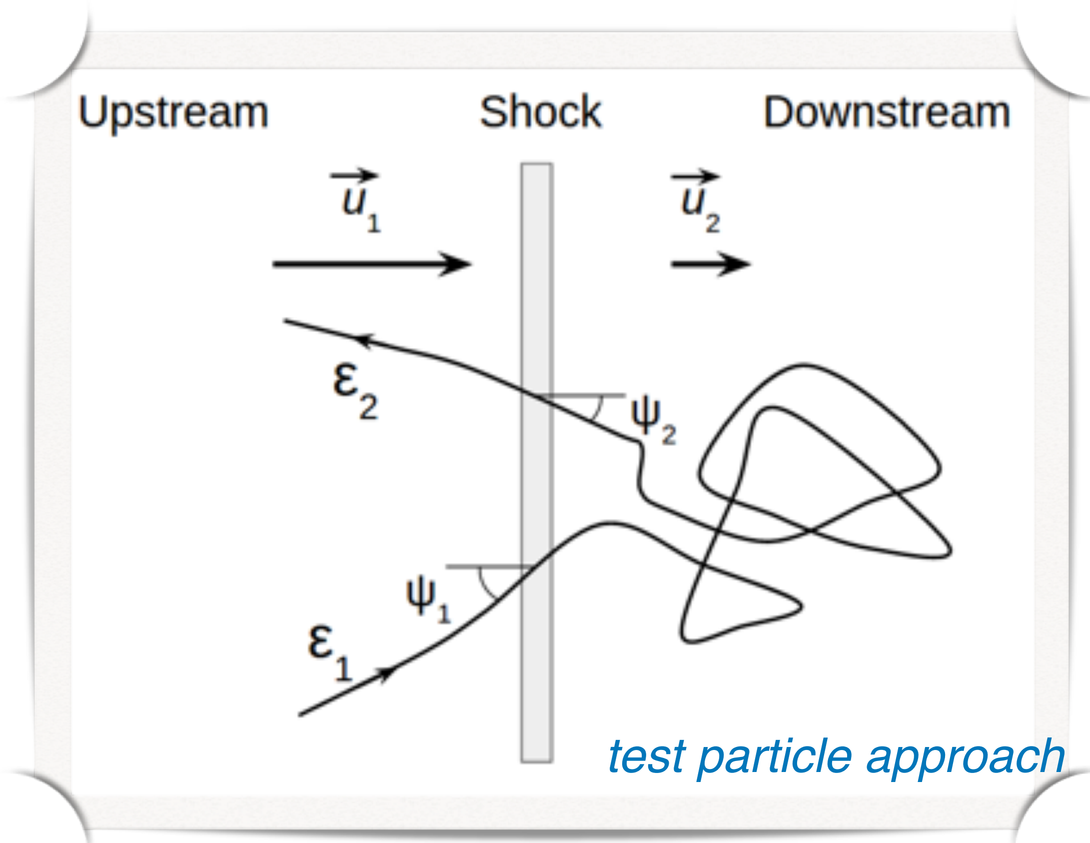

power-law particle spectrum: $N(E) \sim E^{-p}$

spectral index: $p = \frac{r+2}{r-1}$

compression ratio: $r = \frac{u_1}{u_2} = \frac{\Gamma_{\rm ad}+1}{\Gamma_{\rm ad}-1+2/M_{\rm s}^2}$

$r(\Gamma_{\rm ad}=5/3, M_{\rm s}=3) = 3$

$p(r=3) = 2.5$

- electron and proton acceleration (possible production of UHECRs, E >10^{19} eV)
- radiation emission is governed by the efficiency of CR acceleration, that is determined by the injection processes
- particle injection is poorly known for galaxy cluster conditions

radio spectral index: ν^{α}

$\alpha = (1-p)/2$

$M_{\rm s} \simeq 4.6$

$r \simeq 3.5$

$p \simeq 2.2$

$\alpha \simeq -0.6$

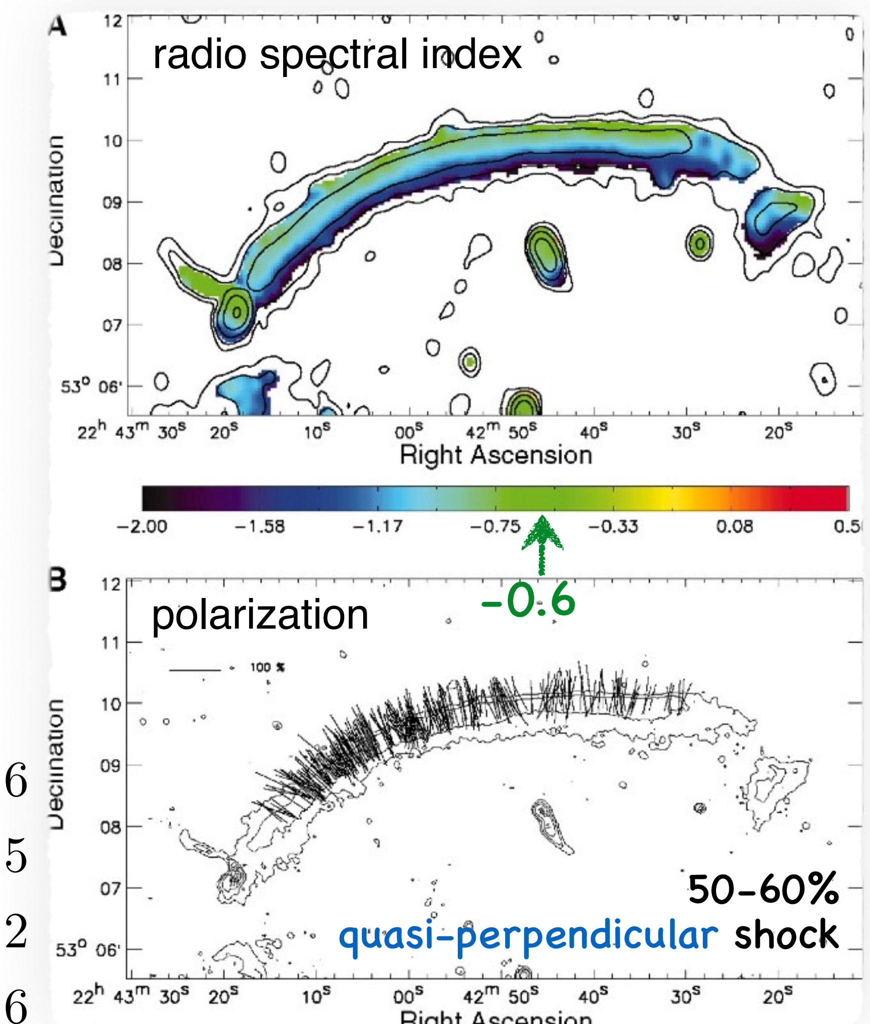

van Weeren et al. (2010)

Particle injection (pre-acceleration) to DSA

DSA

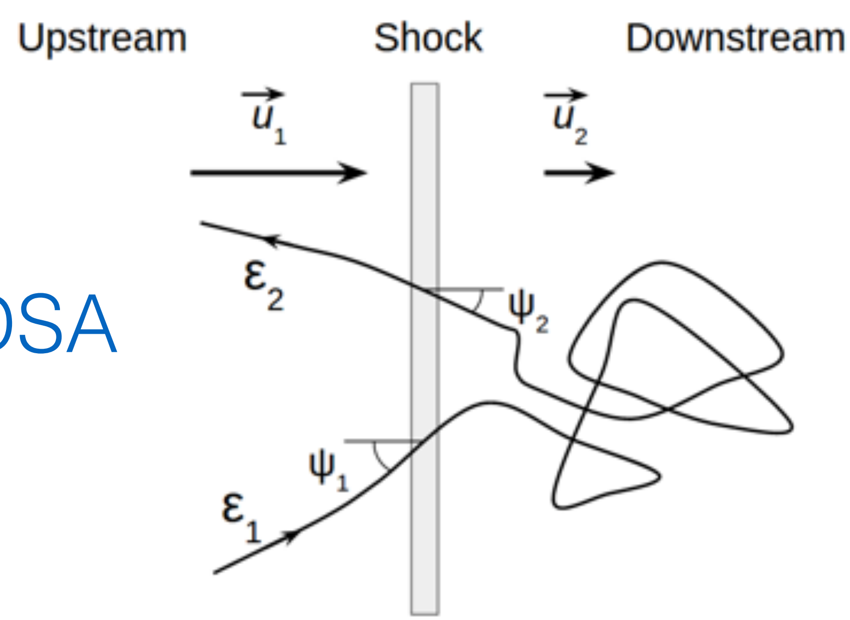

$d_{sh} \sim (1\text{-}100)\ \lambda_{gi}$

$r_g(\varepsilon_{inj}) > d_{sh}$

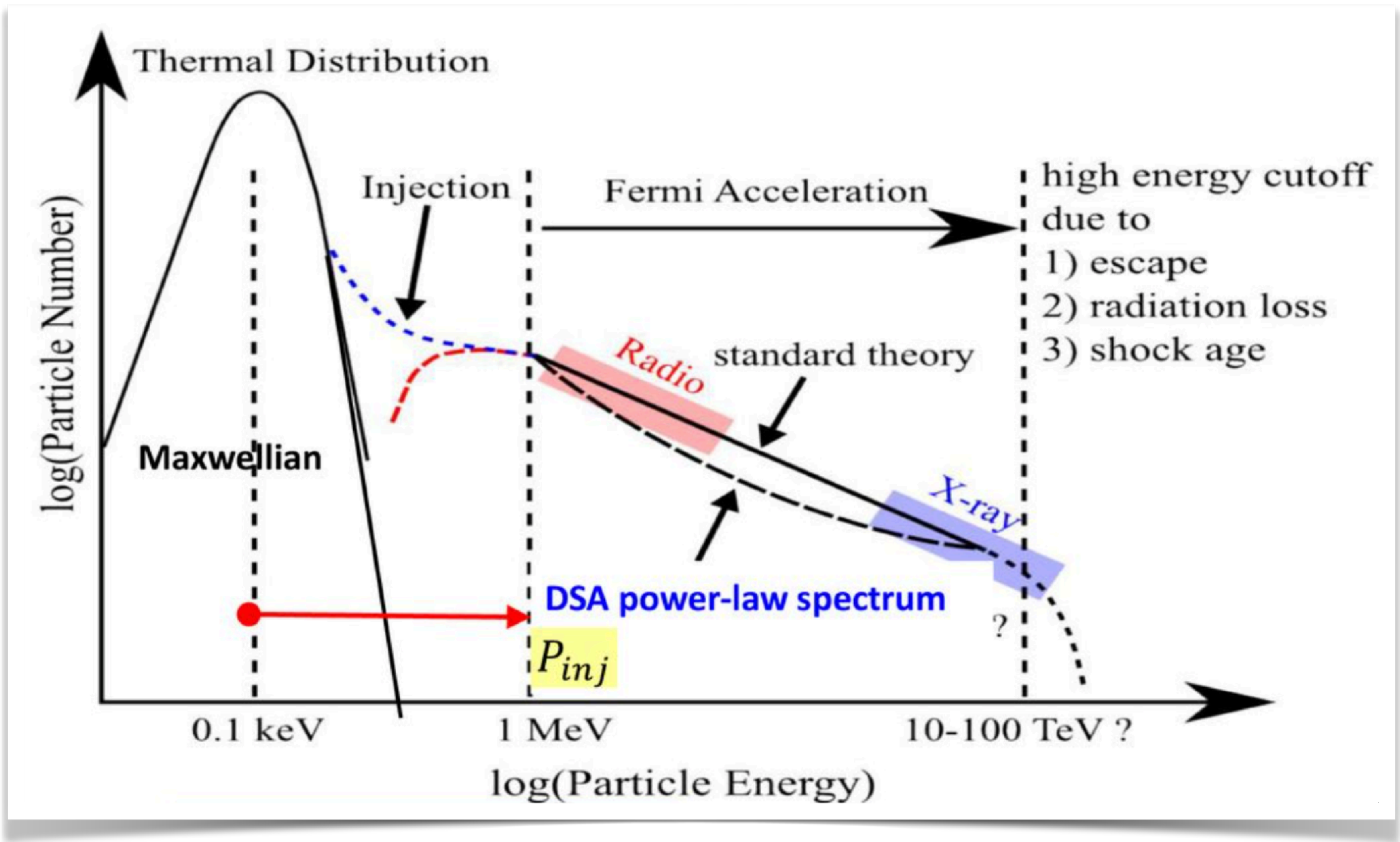

Nonrelativistic shocks in space

$$v_{\rm sh}/c \ll 1$$

- cosmic shocks are in most cases collisionless - plasma particles interact collectively via long-range electromagnetic forces and nonlinearly couple with plasma waves
- shock physics is governed by ion/electron reflection at the shock ramp and plasma instabilities excited through drifts in the shock and in interactions of reflected particles with upstream plasma
- particle acceleration at collisionless shocks depends on various parameters (sonic and Alfvenic Mach number, plasma beta, shock speed, shock obliquity,…)
- studies of microphysical shock structure evolution and particle acceleration require a fully kinetic approach, well beyond fluid (MHD) description

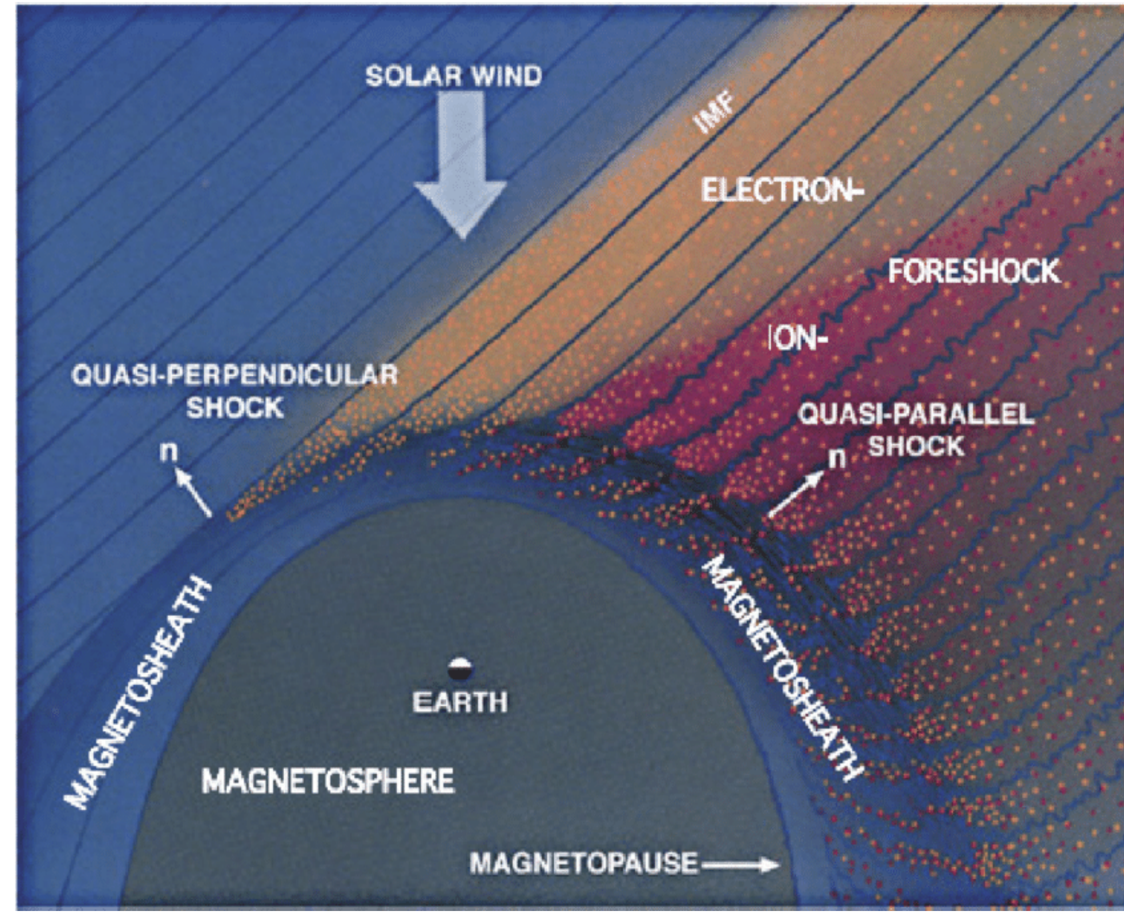

Shock obliquity

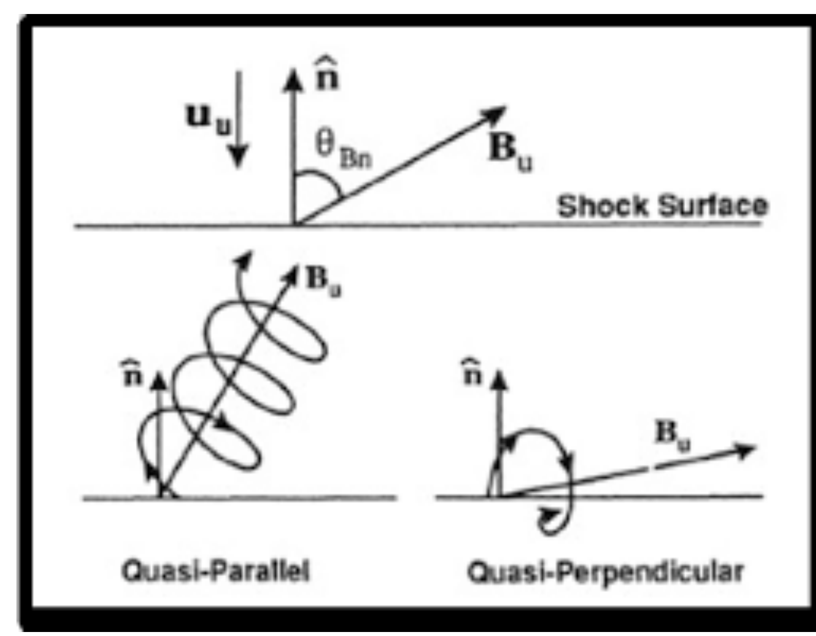

Microstructure of a quasi-perpendicular (high Mach) number shock

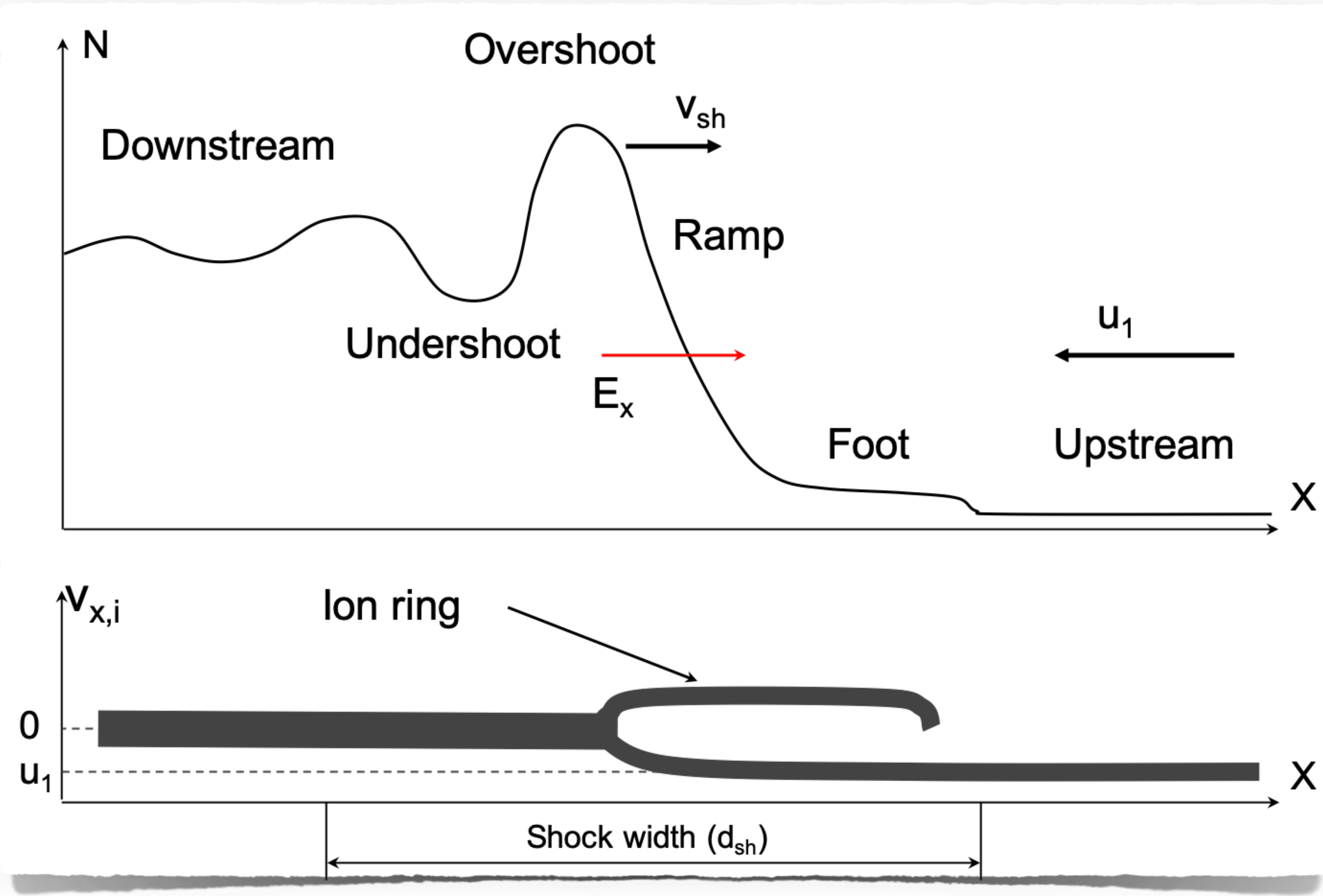

Microstructure of a quasi-perpendicular high Mach number shock

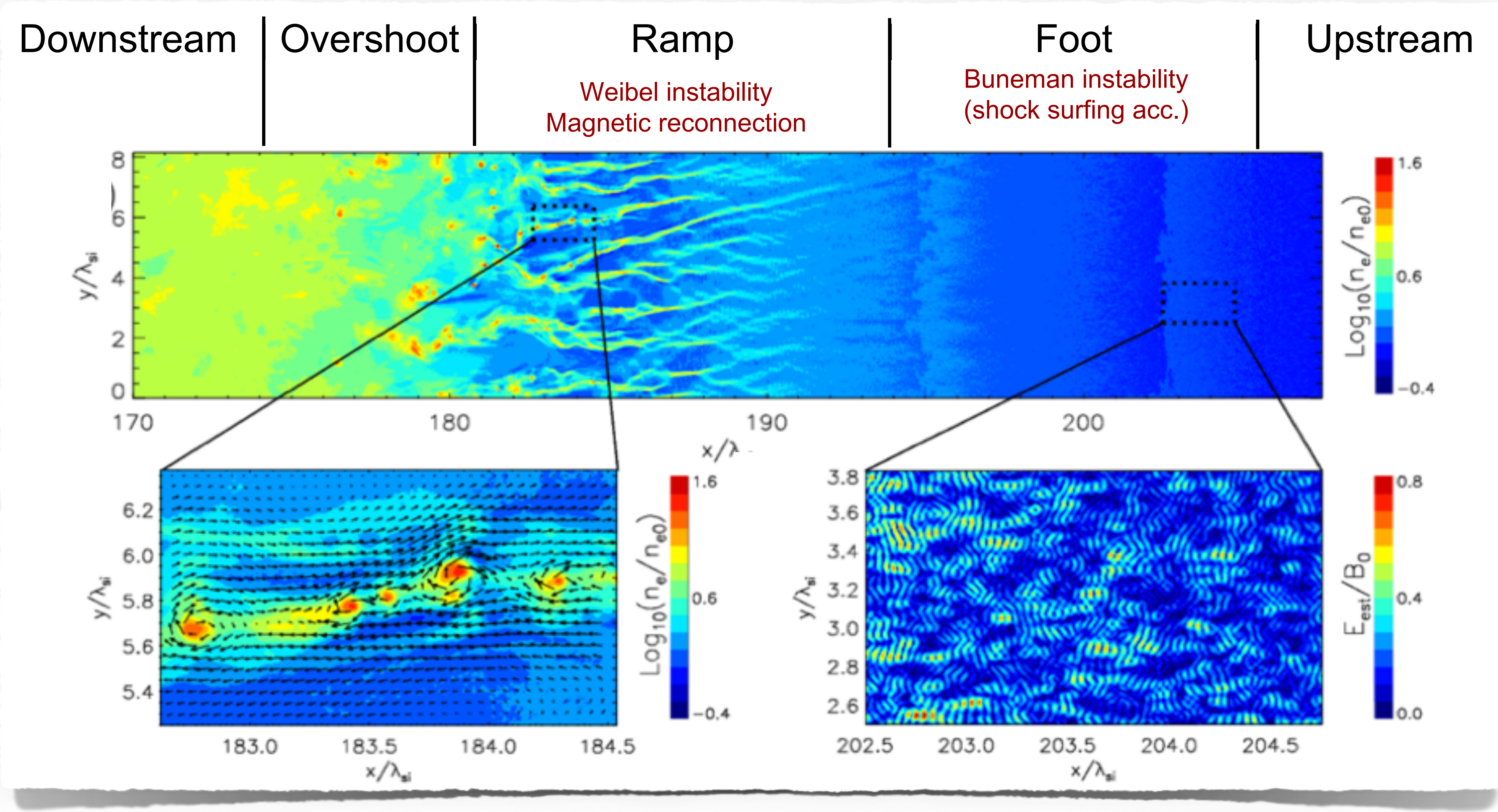

PIC simulation result; courtesy: A. Bohdan

Method of Particle-In-Cell Simulations

- Fully self-consistent description of collisionless plasma:
  - Vlasov equation (kinetic theory; time evolution of particle distribution function *f*(***x***,***v***,*t*) in phase-space) + Maxwell's equations

- Particle-In-Cell modeling - an *ab-initio* method of Vlasov equation solution through:
  - integration of Maxwell's equations on a numerical grid
  - integration of relativistic particle equations of motion in collective self-consistent EM field

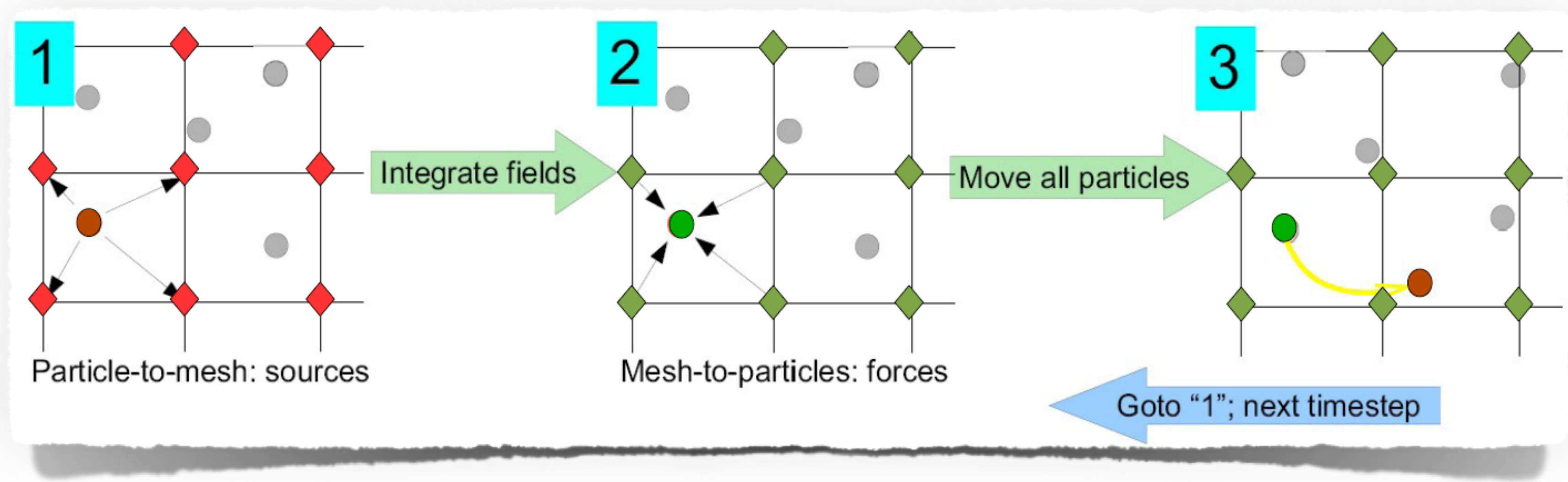

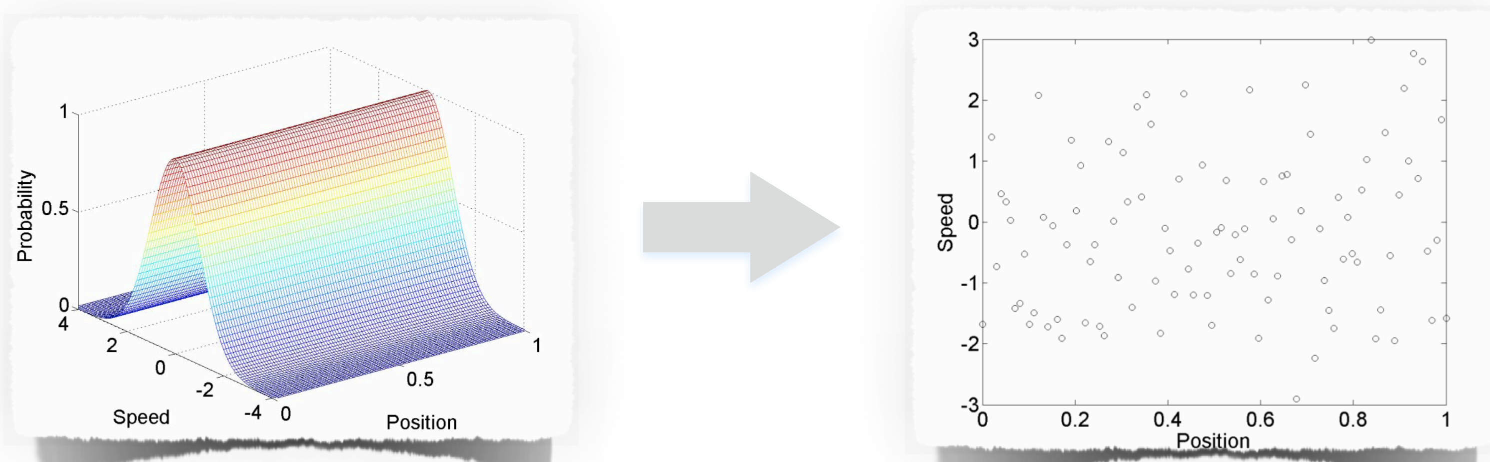

Particle distribution function represented by macroparticles on a numerical grid.
(Macroparticles represent a small volume of particle phase-space; equations of motion as for realistic particles)

PIC Numerical Model

Definition of plasma: $L \gg \lambda_D$

Typical astrophysical system $N_D >> 1$ (e.g. ionosphere $N_D \sim 10^4$)

Basic plasma condition: $\frac{\langle E_{kin} \rangle}{\langle E_{pot} \rangle} \gg 1$

$$\frac{\langle E_{kin} \rangle}{\langle E_{pot} \rangle} \sim 6\pi N_D^{2/3}$$

Is $N_D \sim 10$ *enough*? How else obtain $N_D \gg 1$?

$$\frac{\nu_c}{\omega_{pe}} \sim \frac{1}{N_D} \ln N_D$$

- numerical grid for EM fields
- finite-size particle shape model - effective elimination of short-range forces

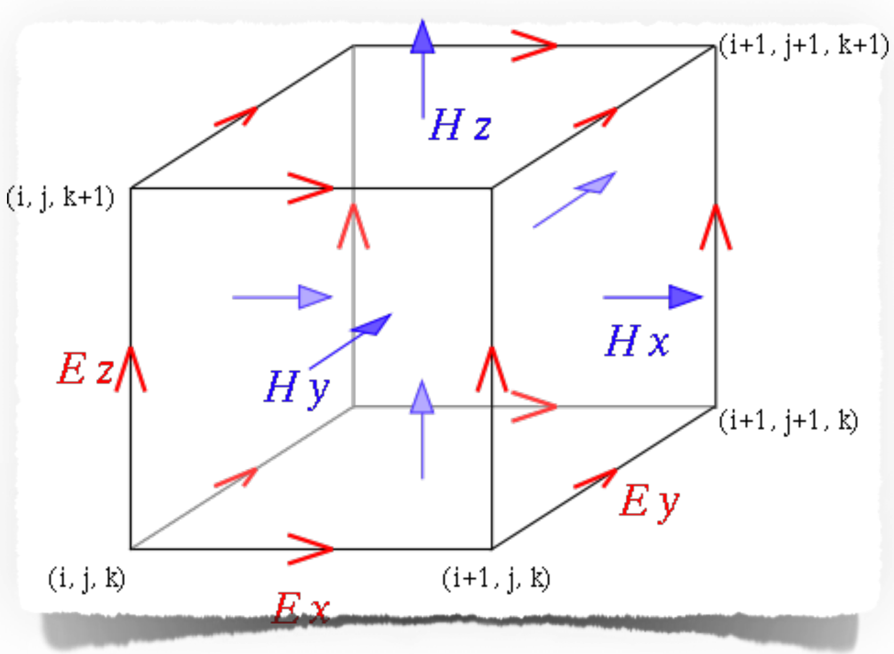

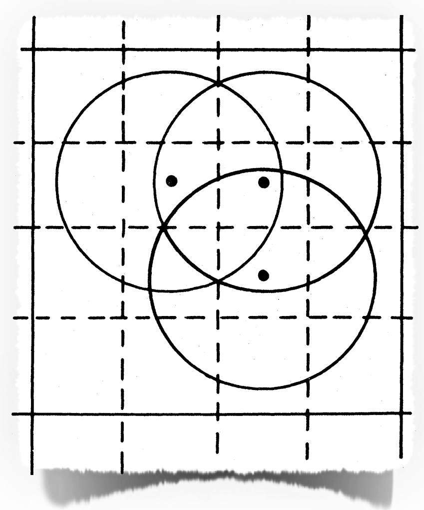

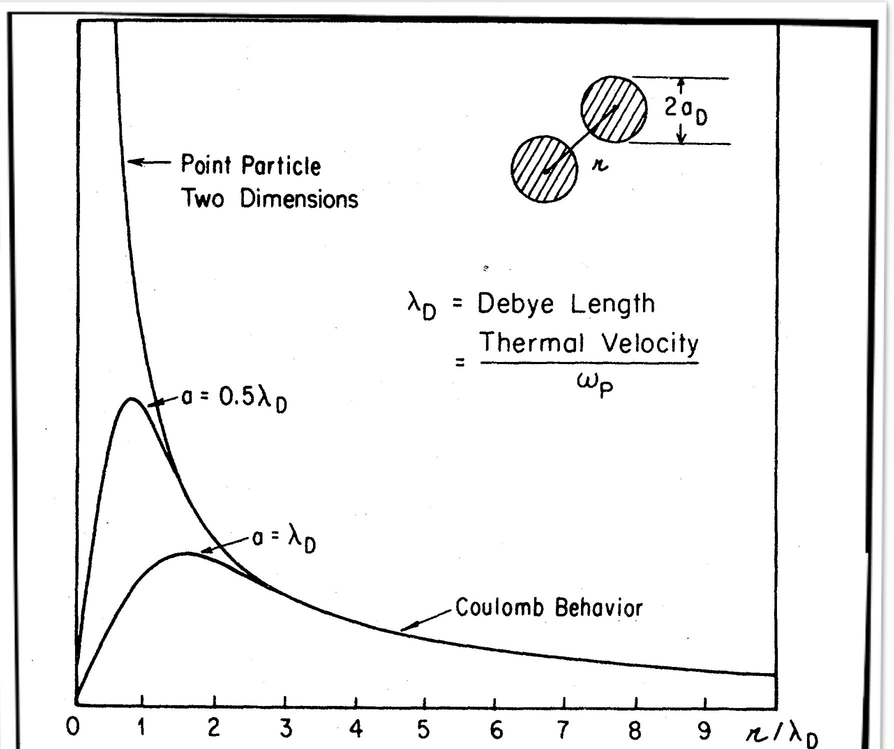

FIG. 2. Force law between finite-size particles in two dimensions for various sized particles. A Gaussian-shaped charge-density profile was used.

Dawson '83

Scales, units, definitions [SI]

$$\text{Debye length}: \quad \lambda_D = \sqrt{\epsilon_0 k_B T / e^2 N_e}$$

$$\text{electron plasma frequency}: \quad \omega_{\mathrm{pe}} = \sqrt{\mathrm{e^2 N_e / \epsilon_0 m_e}}$$

$$\text{electron/ion skindepth}: \quad \lambda_{\mathrm{se}} = \mathrm{c}/\omega_{\mathrm{pe}}, \ \lambda_{\mathrm{si}} = \mathrm{c}/\omega_{\mathrm{pe}}$$

$$\lambda_{si} = \lambda_{se}\sqrt{m_i/m_e}$$

$$\text{ion cyclotron frequency}: \quad \Omega_i = eB_0/m_i$$

$$\text{ion gyroradius}: \quad r_g \equiv v_0/\Omega_i = \frac{v_0}{v_{sh}} M_s \lambda_{si} \sqrt{\beta\Gamma/2}$$

$$\text{plasma beta}: \quad \beta = \beta_e + \beta_i = \frac{2\mu_0 (N_e + N_i) k_B T_0}{B_0^2}$$

Electron injection at shocks in high beta plasmas: Shock Drift Acceleration (SDA)

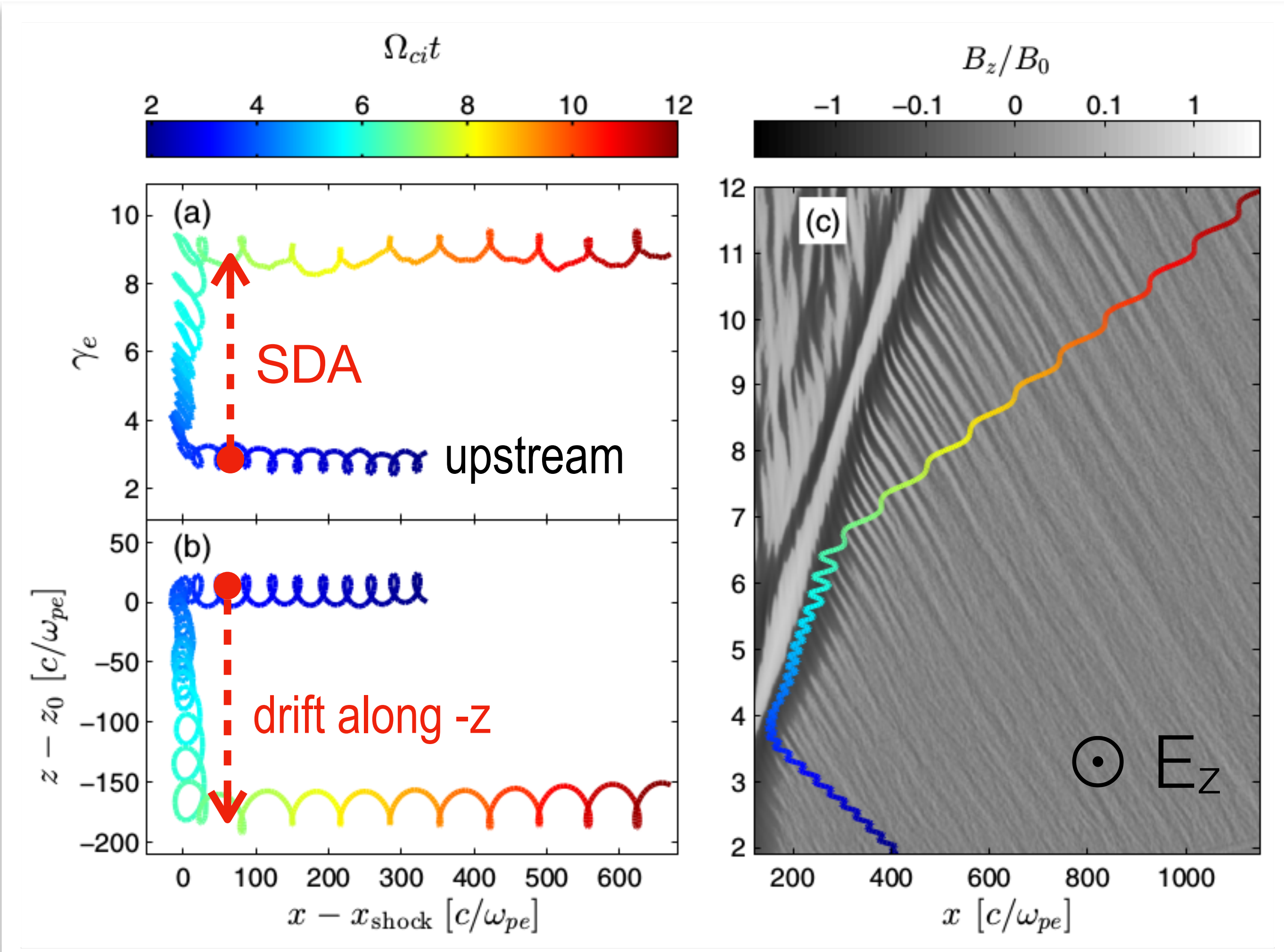

Guo et al. 2014 (2D)

- particles gain energies from the motional electric field while drifting along the shock surface due to the magnetic field gradient
- some particles can be reflected from the shock back upstream (magnetic mirror effect) and form non-thermal upstream plasma component
- works at subluminal shocks: $v_t \leq c$
- acceleration time: $\sim \Omega_i^{-1}$
- energy gain:

$$\Delta\gamma_{\mathrm{SDA}} = \frac{-e}{m_e c^2} \int E_z \, dz$$

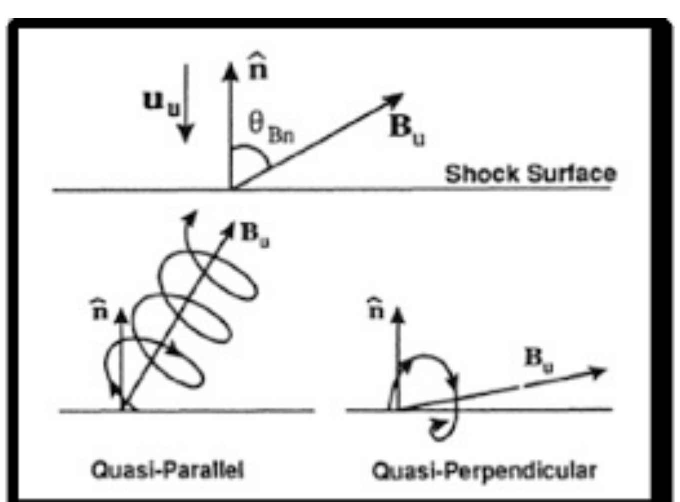

de Hoffman-Teller velocity:

$$v_t = u_{\mathrm{sh}}^{\mathrm{up}} / \cos\theta_{\mathrm{Bn}}$$

SDA - example upstream spectrum

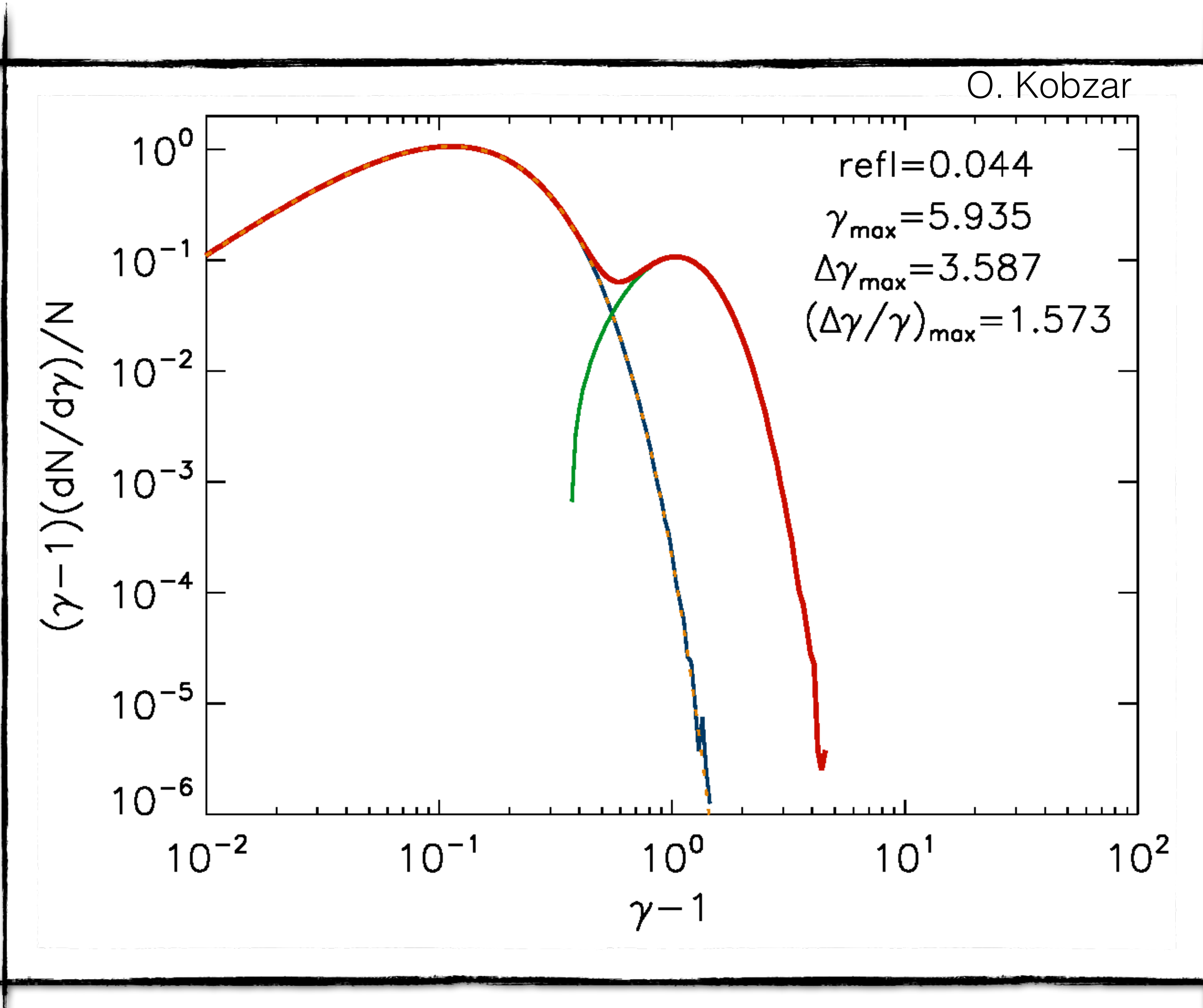

Previous work: multiple SDA cycles at quasi-perpendicular shocks

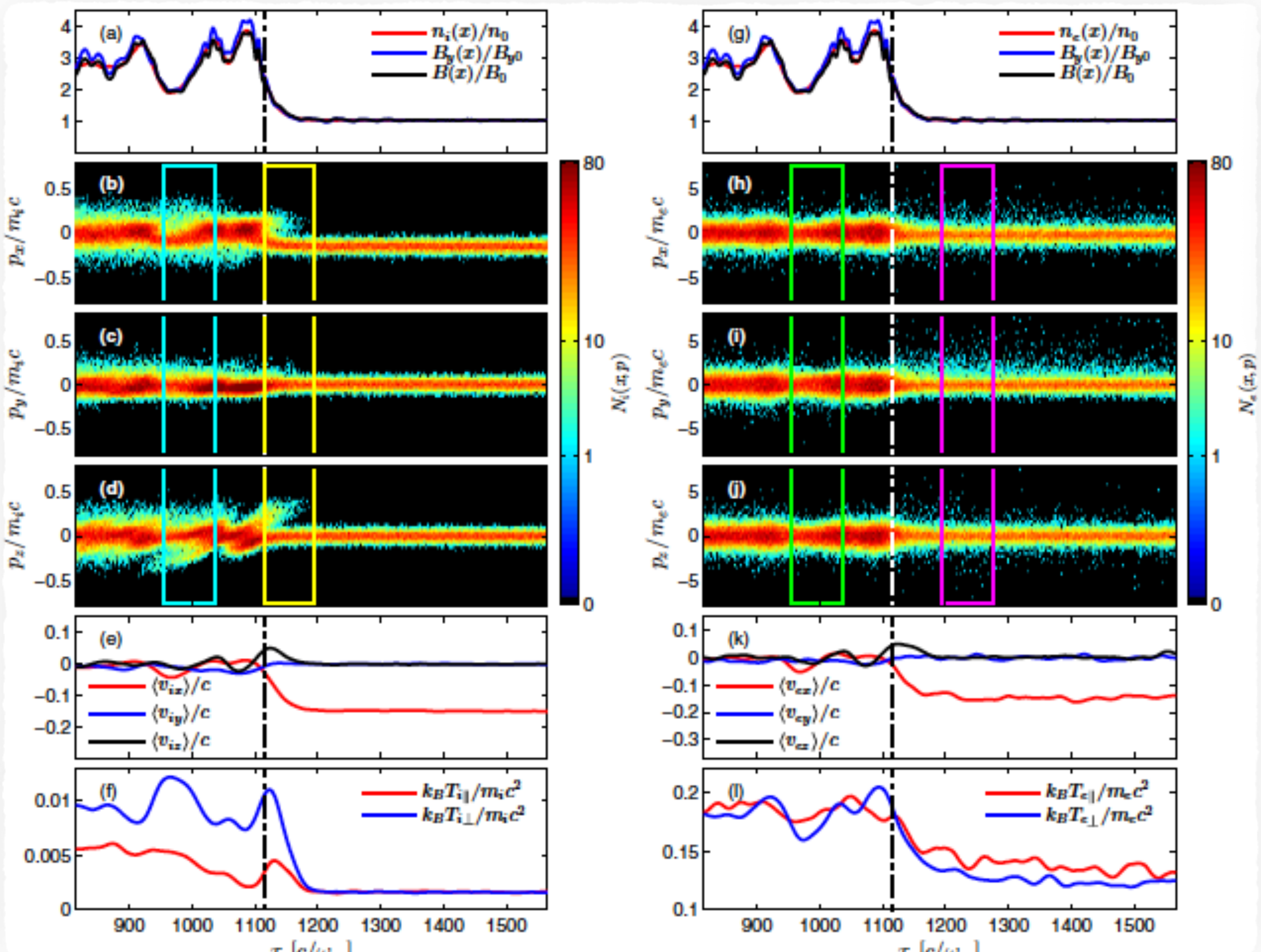

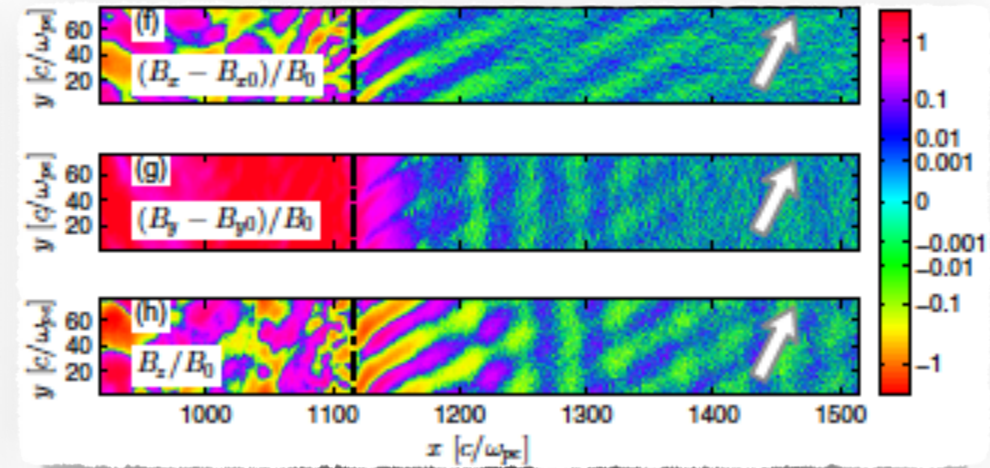

- shock-reflected energetic electrons propagating upstream self-generate magnetic waves (oblique electron firehose instability (EFI) due to electron temperature anisotropy)

2D3V, M_A=8.2, M_s=3, ϑ=63°, m_i/m_e=100, v_0=0.15c, β=20; Guo et al. 2014

Previous work: multiple SDA cycles at quasi-perpendicular shocks

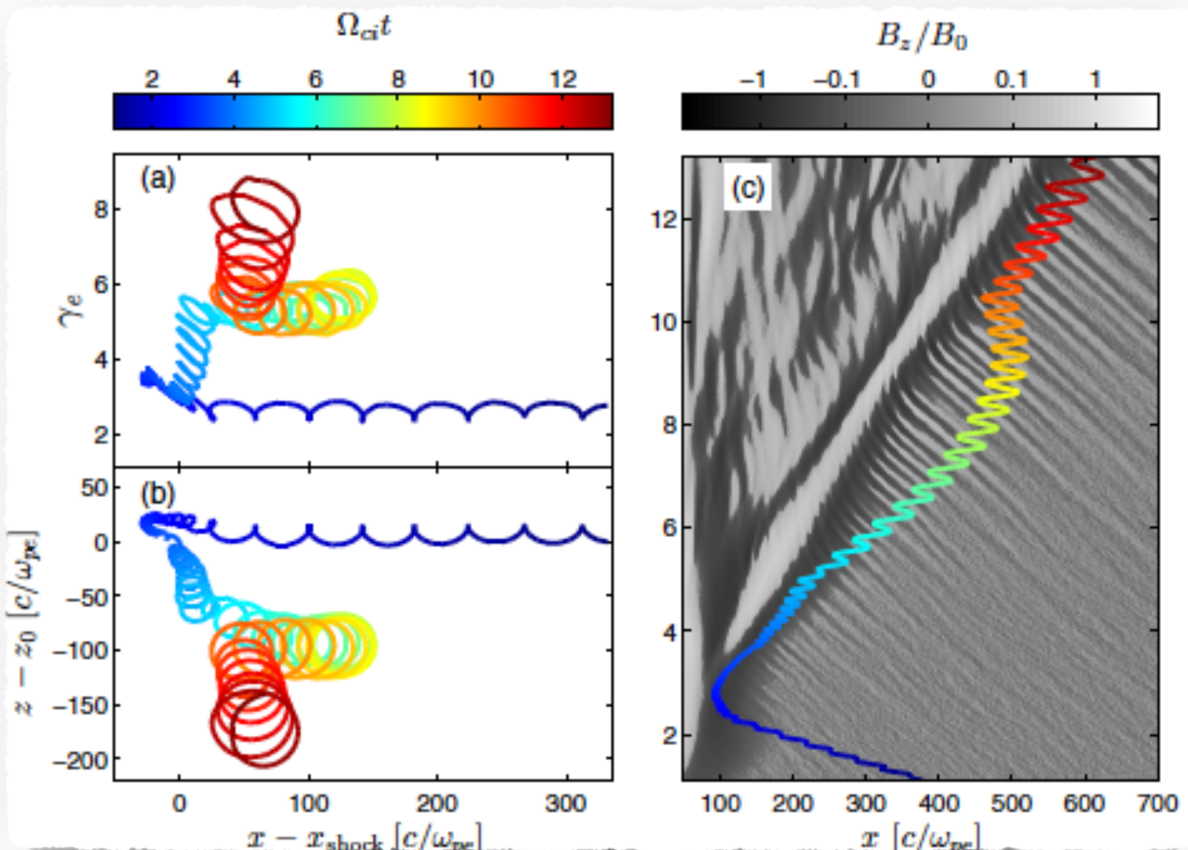

- SDA-reflected electrons scattered back towards shock by upstream self-generated waves - DSA-like process
- formation of upstream power-law spectra
- more effective at high β
- $\gamma_{max} \ll \gamma_{inj}$?

Matsukiyo et al. 2011 (1D)
Guo et al. 2014 (2D)
Kang et al. 2019 (2D)

upstream

downstream

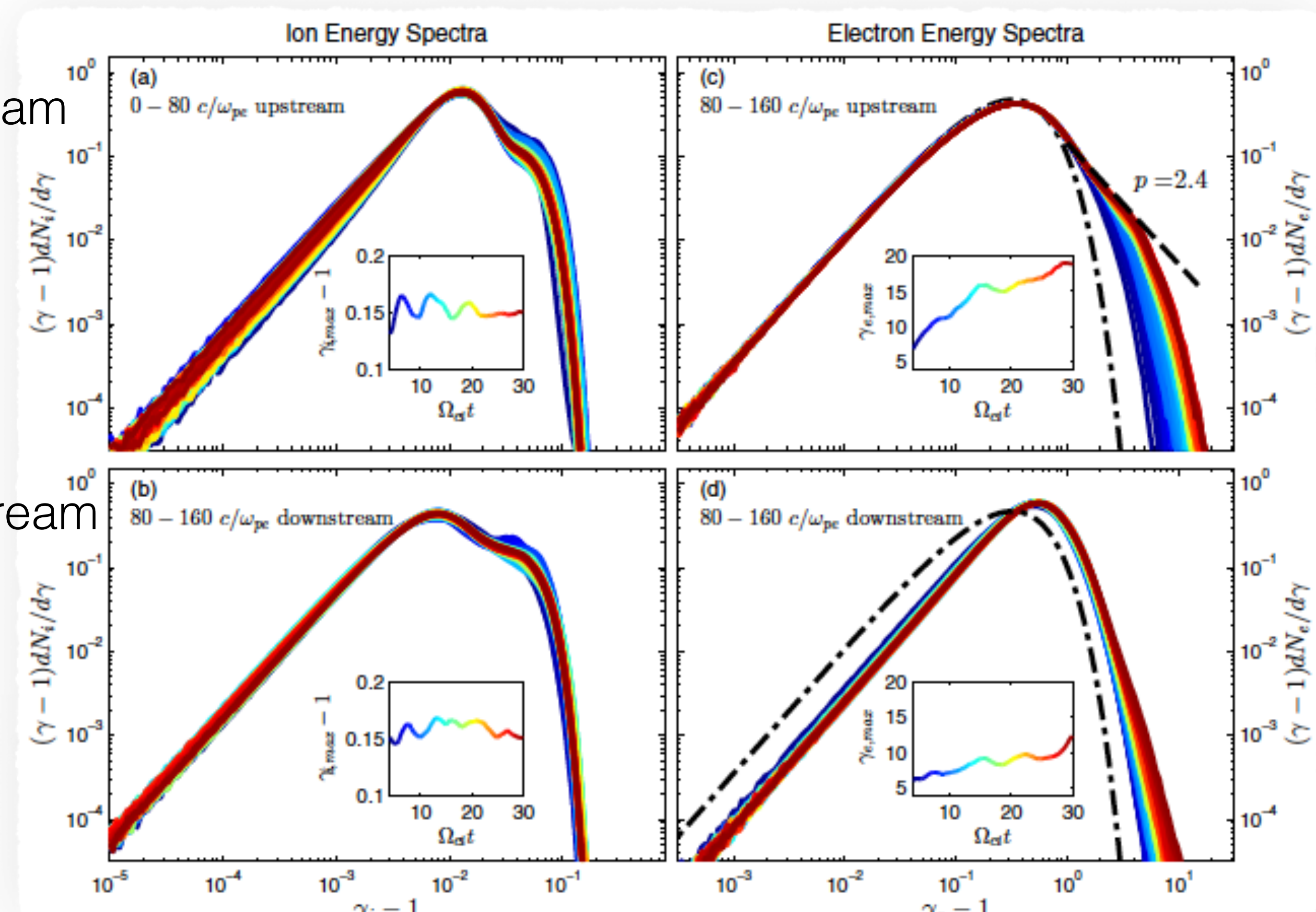

Effects of the shock rippling (large-scale 2D simulations)

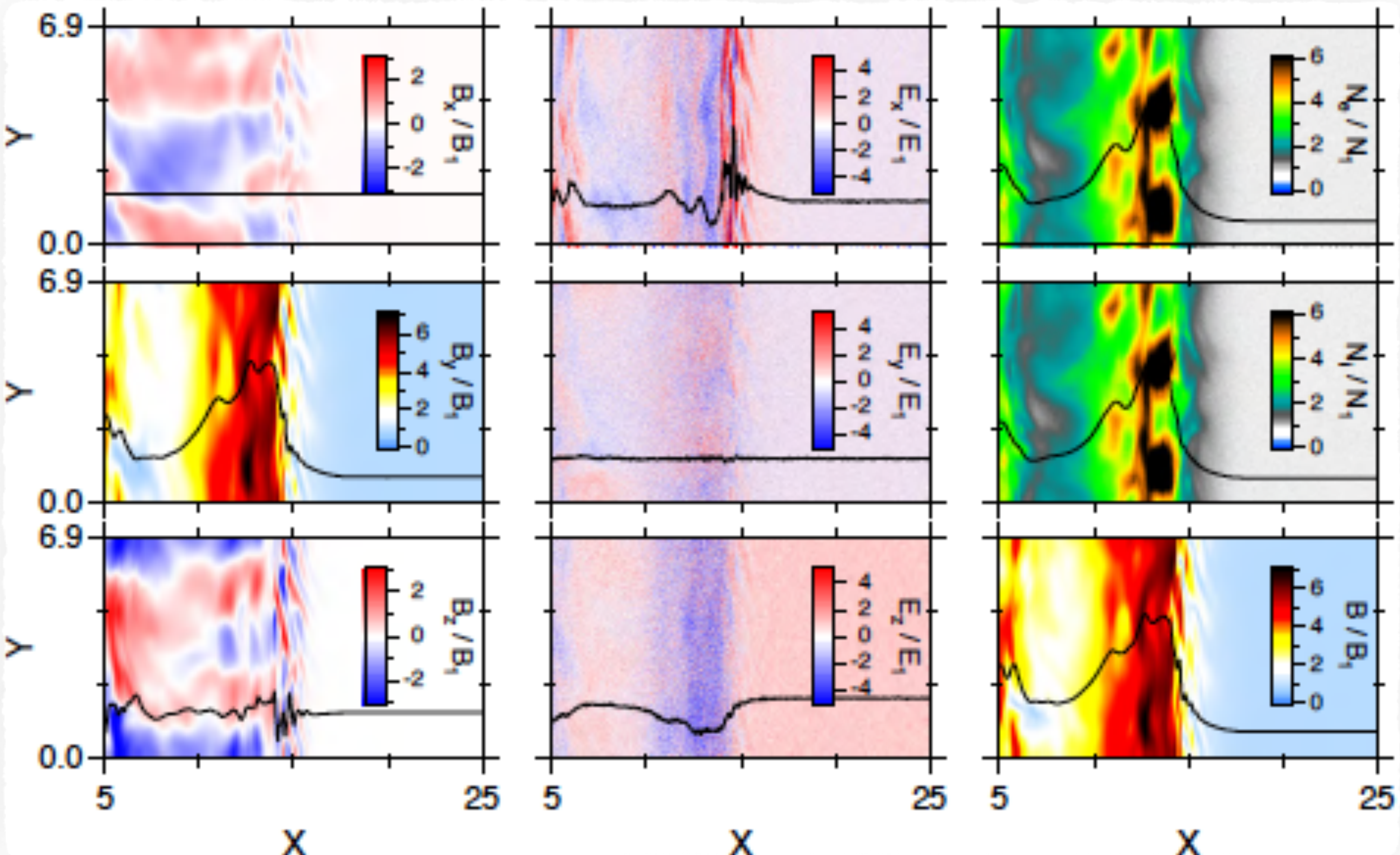

- no reflected electrons because of ion-scale shock ripples
- SDA does not work
- acceleration by scattering on the waves in the shock transition instead
- if the same shock rippling mechanism operates for conditions assumed in Guo et al. 2014 and Kang et al. 2019, then their simulations might have not been able to resolve it

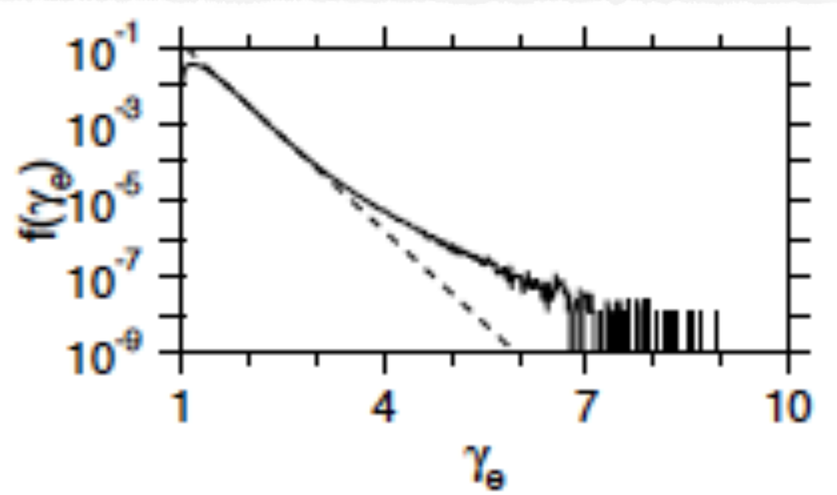

spectrum in overshoot

relatively low β=3, Matsukiyo & Matsumoto 2015

Large-scale effects of the shock rippling on electron pre-acceleration with PIC simulations

Kobzar O., et al., ApJ 2021
Fułat K., M.Sc. thesis (2021)
Kobzar O., et al., 2024 in prep.
(see also Matsukiyo & Matsumoto 2015)

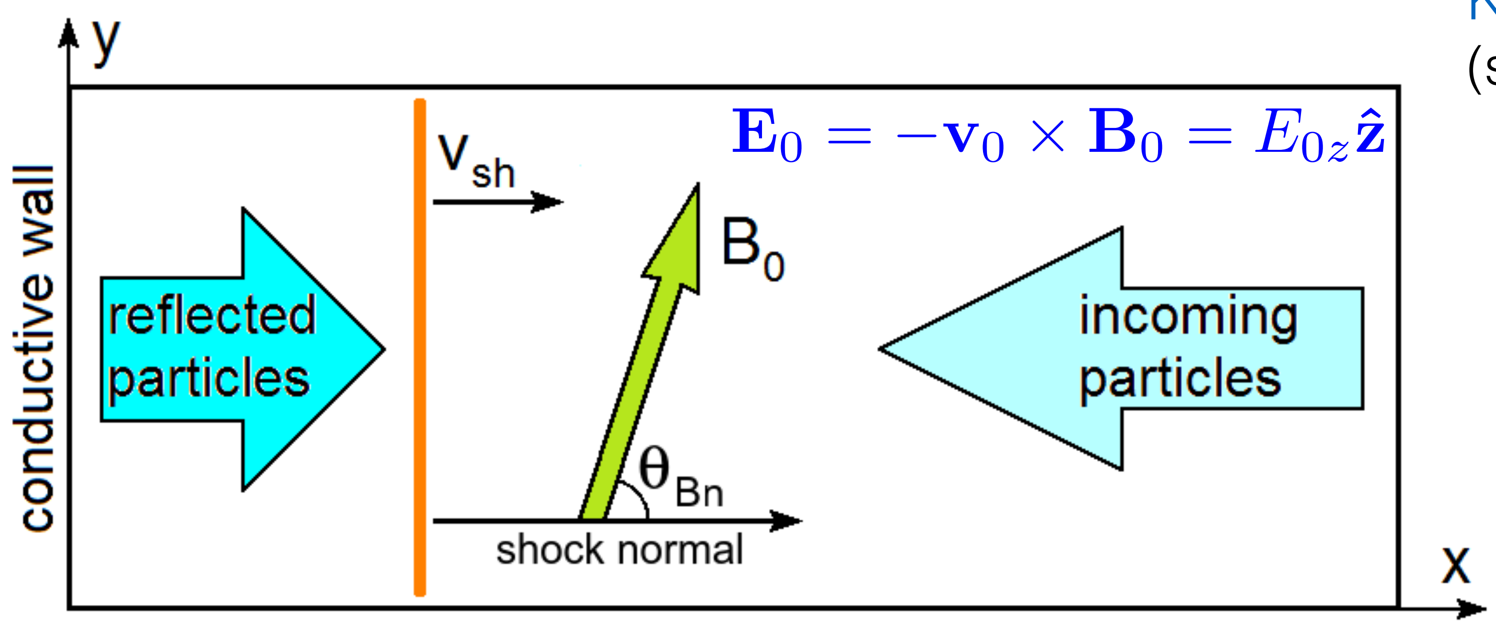

Large-scale 2D3V Particle-In-Cell (PIC) simulations

- M_s=3, m_i/m_e=100, v_0=0.1c, β=5, 10, 20, 30 (plasma temperature $k_B T \approx$ 40 keV)
- subluminal shocks: ϑ_{Bn}=75°, 78° ($\vartheta_{cr} \approx$ 81,4°)
- conditions of inefficient EFI mode driving in the laminar shock phase:

$$v_t \gtrsim v_{\rm th,e} \; (v_t = u_{\rm sh}^{\rm up} / \cos\theta_{\rm Bn})$$

$$v_t \approx 1.5 v_{\rm th,e} \; (\theta_{\rm Bn} = 75^o)$$
$$v_t \approx 1.9 v_{\rm th,e} \; (\theta_{\rm Bn} = 78^o)$$

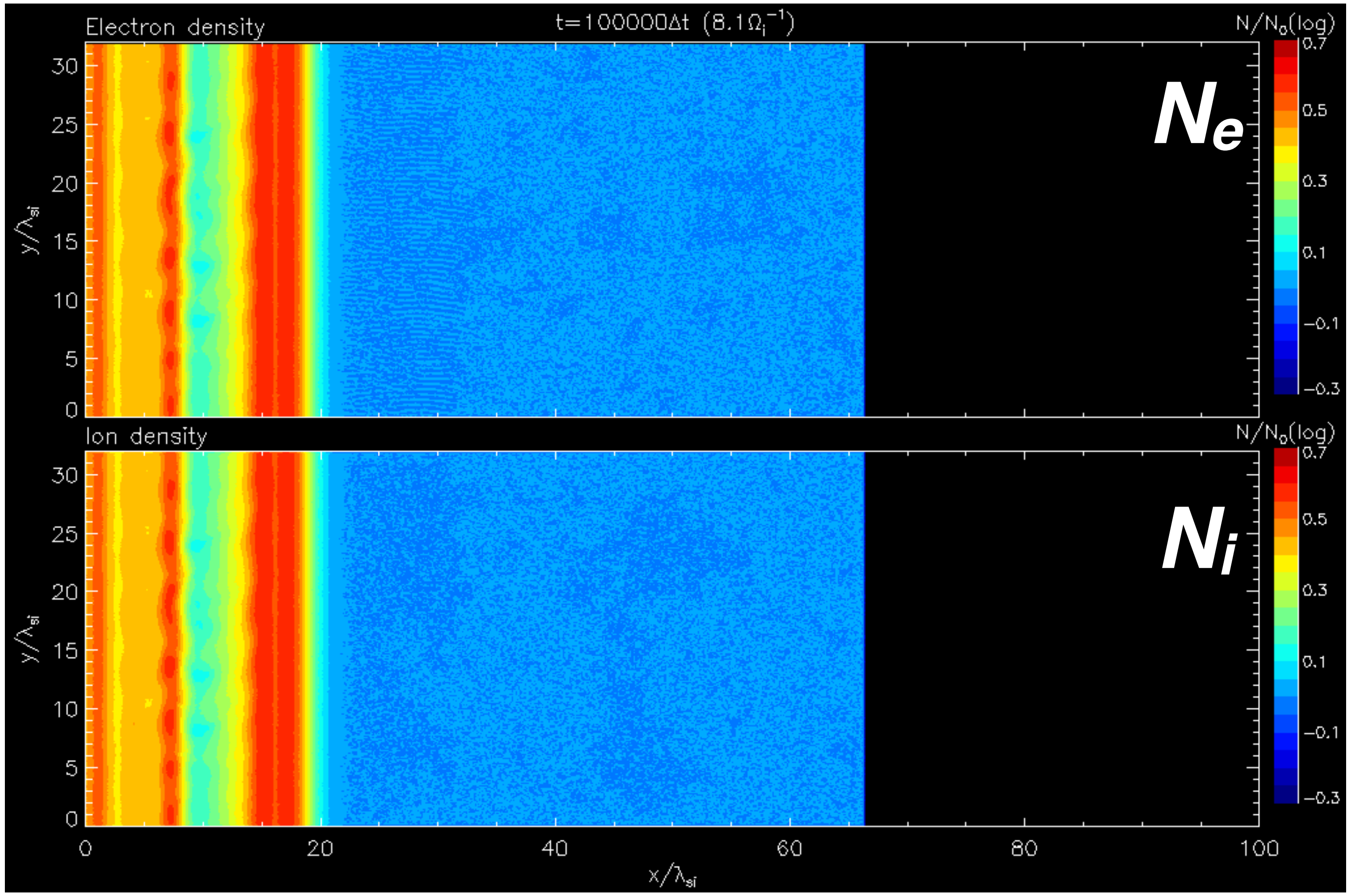

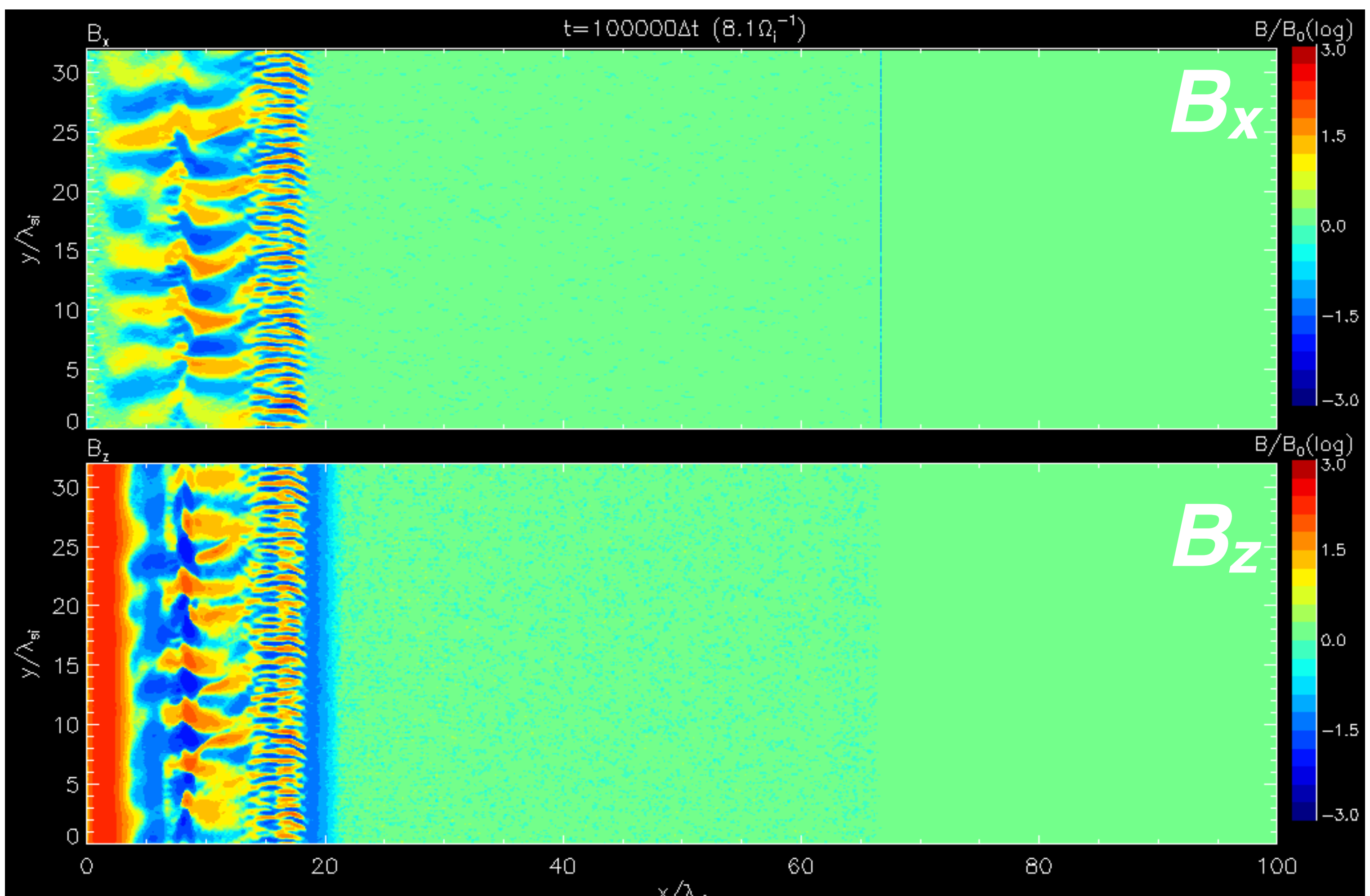

Global shock structure: multi-scale turbulence (β=5, ϑ_{Bn}=75°)

- rippling in the shock transition on different scales (overshoot-undershoot-2nd overshoot)
  - AIC and mirror modes
- short-scale whistler waves in the overshoot
- oblique and perpendicular modes of the electron firehose instability in the upstream, enhanced and modulated by the ripples

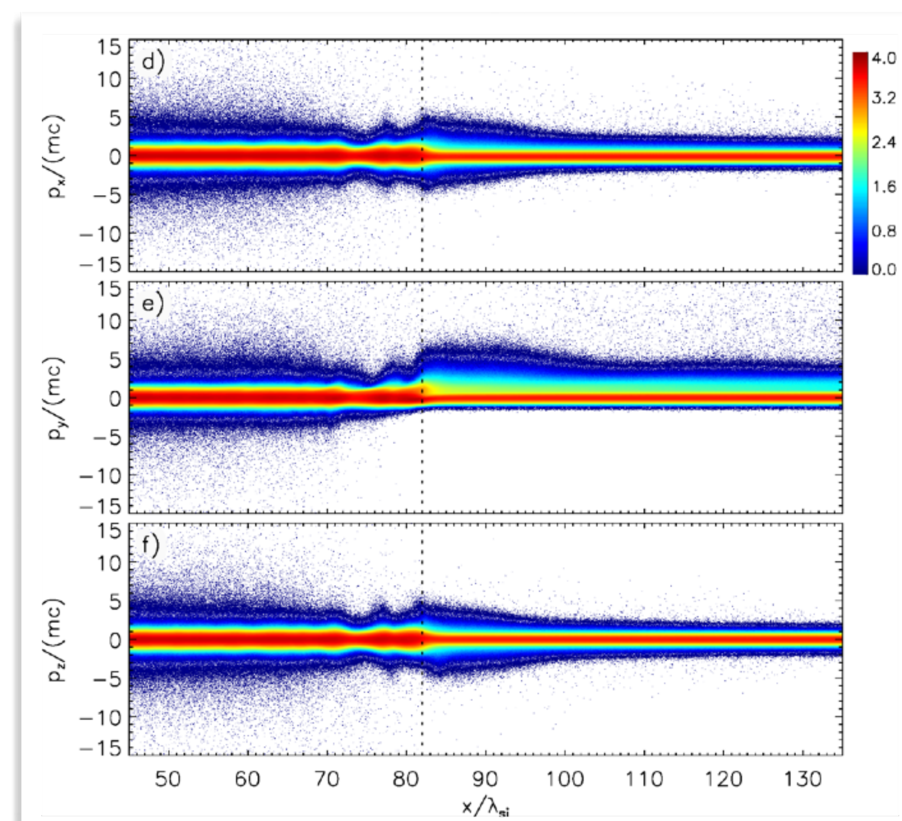

Wave modes

(β=5, ϑ_{Bn}=75°)

- Rippling in the overshoot due to Alfven ion cyclotron (AIC) instability caused by ion temperature anisotropy
- Slowly growing mode at $\lambda_{rip} \approx 16\lambda_{si}$ ($T_{perp}/T_{par} \approx 4.7$)

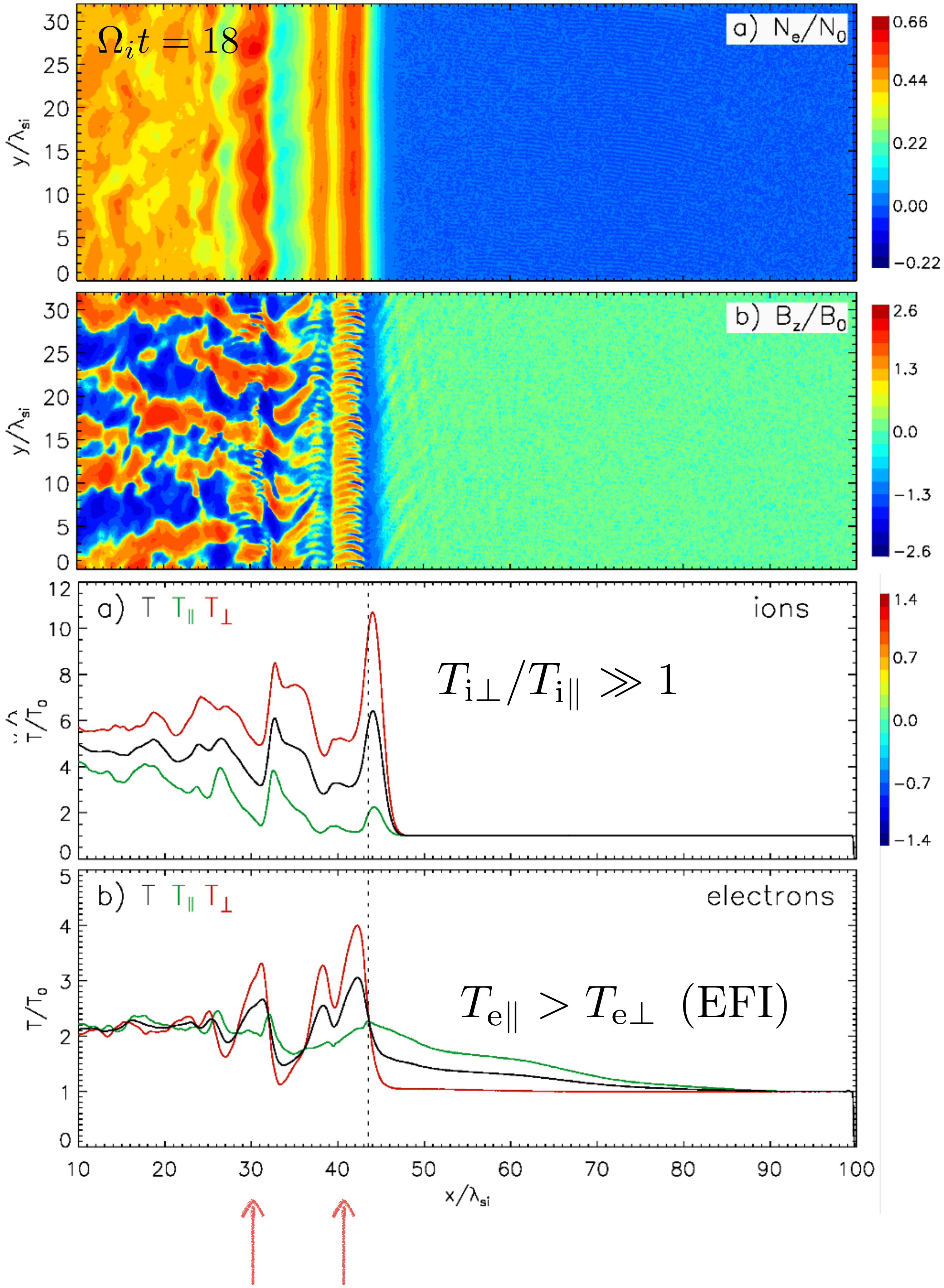

$T_{e\perp} > T_{e\parallel}$ (whistlers)

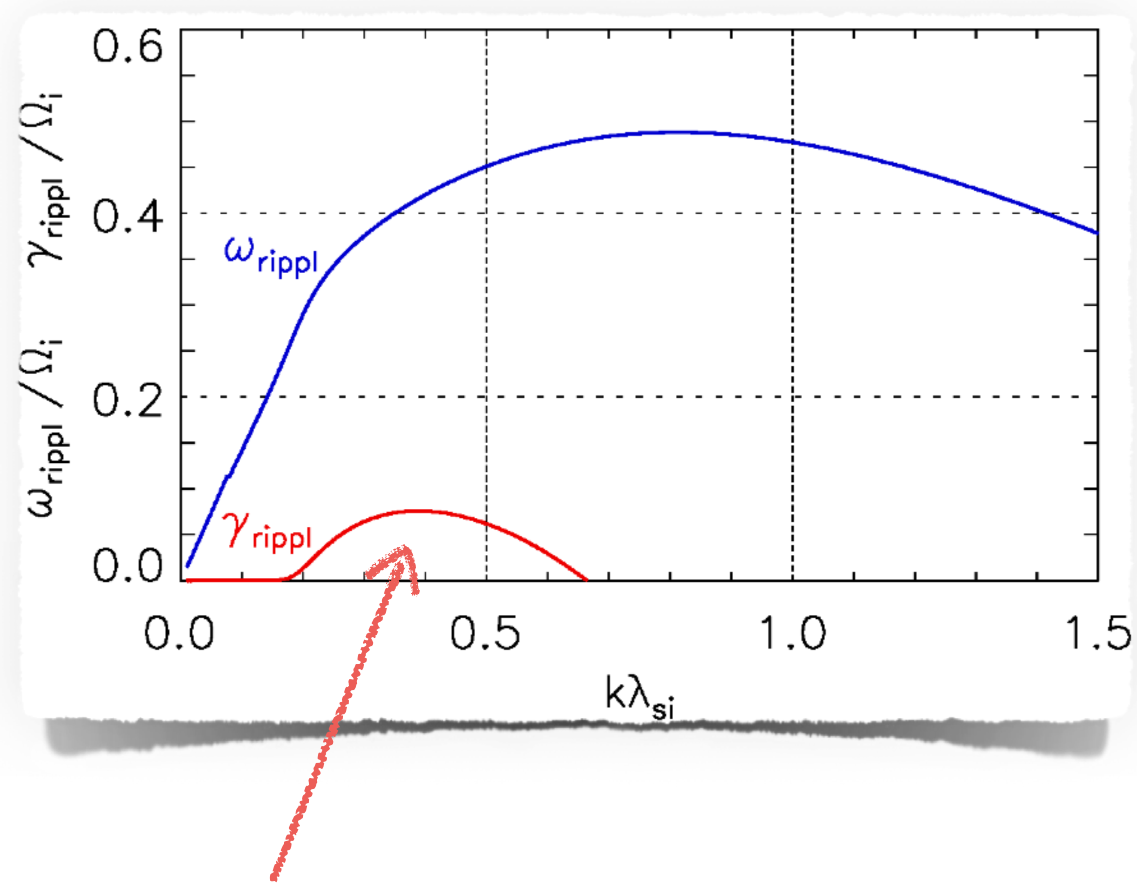

growth rate

Electron spectra – time evolution (β=5, ϑ_{Bn}=75°)

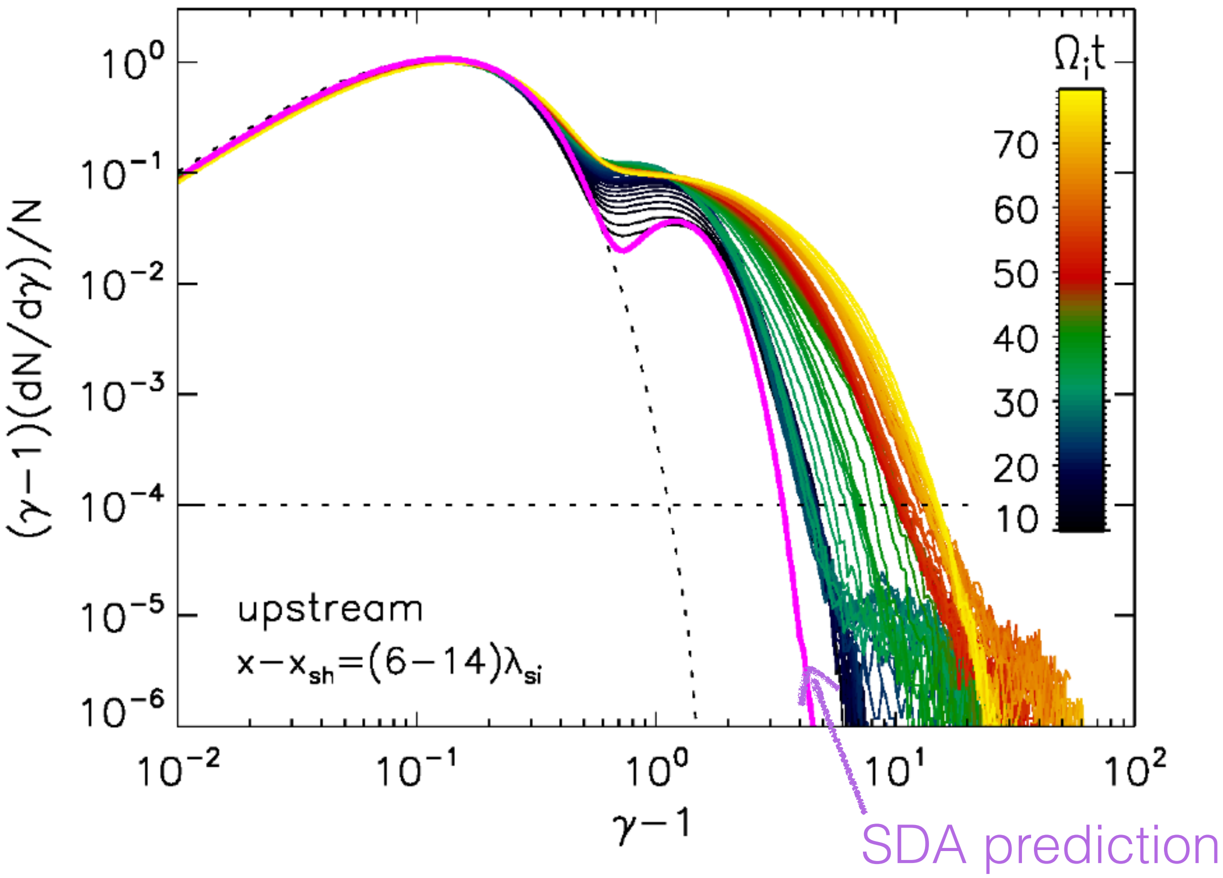

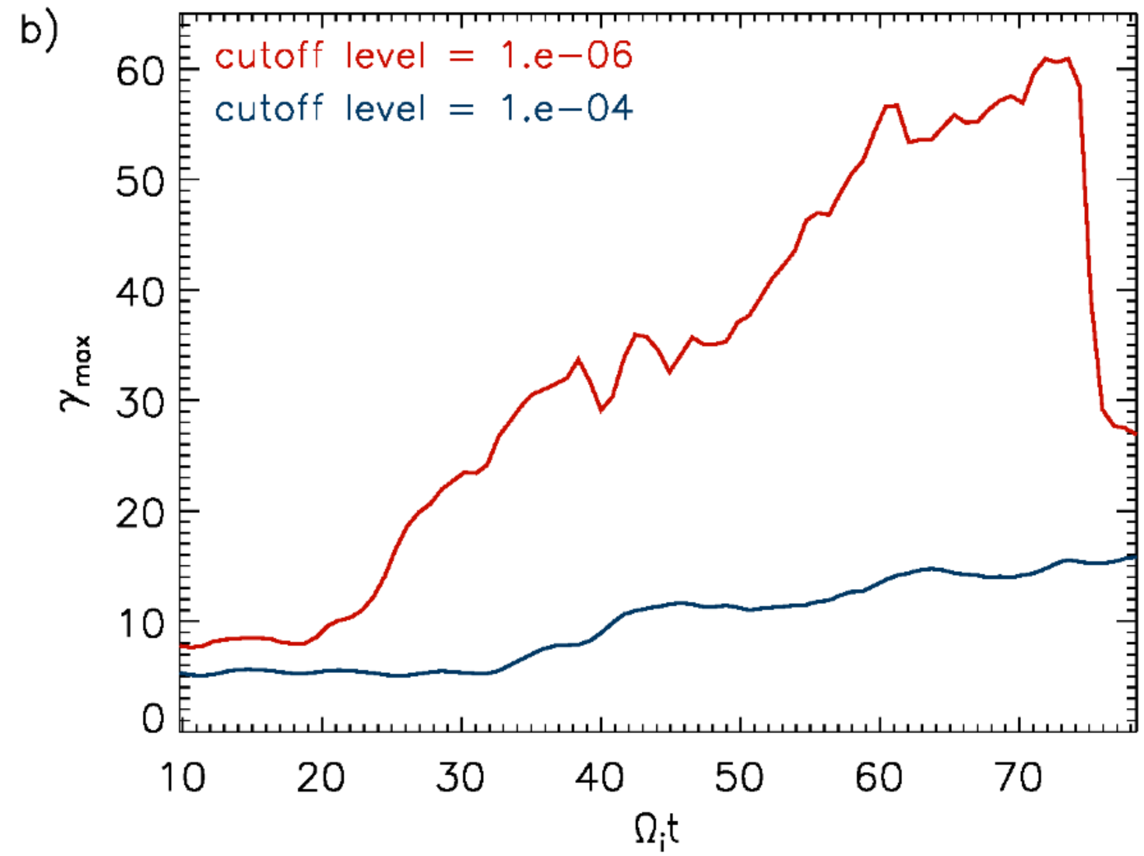

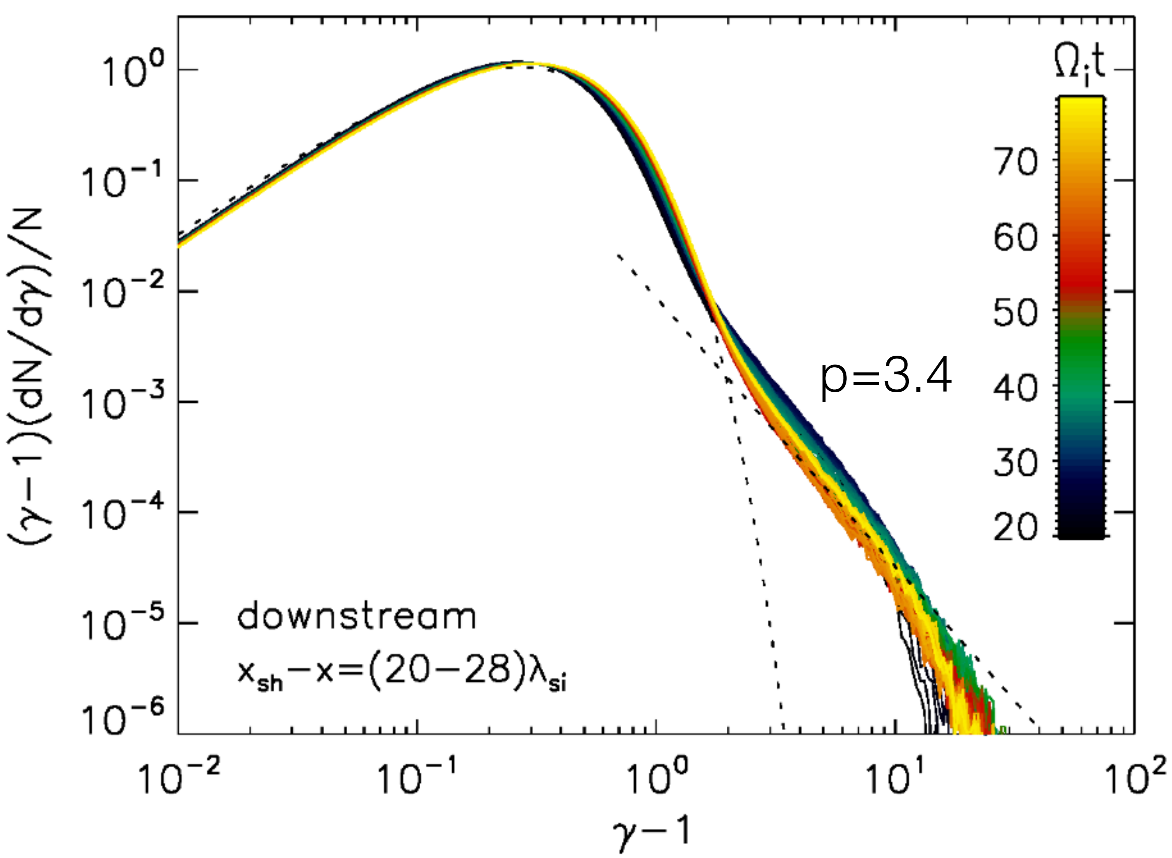

- substantial increase in non-thermal tail production efficiency coincident with the onset of the shock rippling at $\Omega_{ci}t \approx 25$
- limited-range power-law spectra downstream

Electron spectra – injection efficiency (β=5, $\vartheta_{\rm Bn}$=75°)

upstream

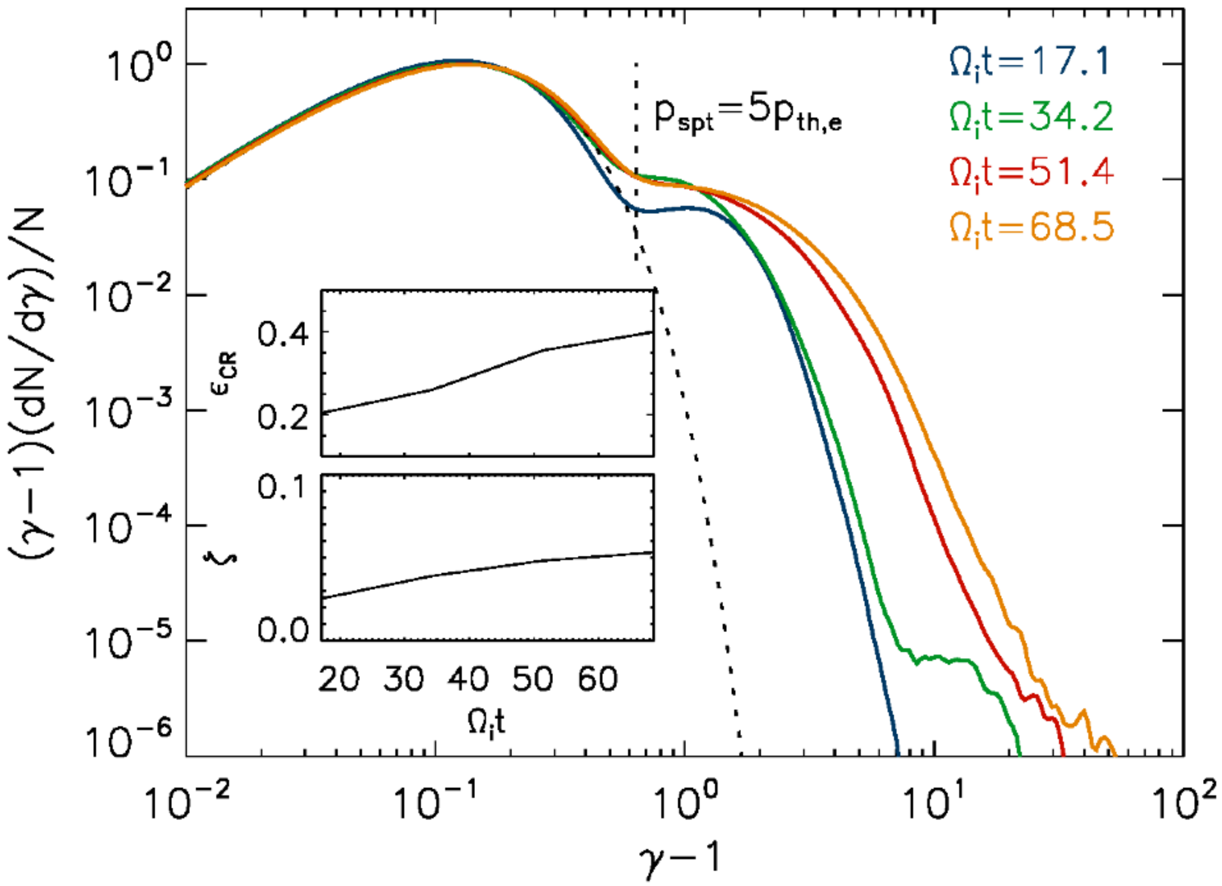

downstream

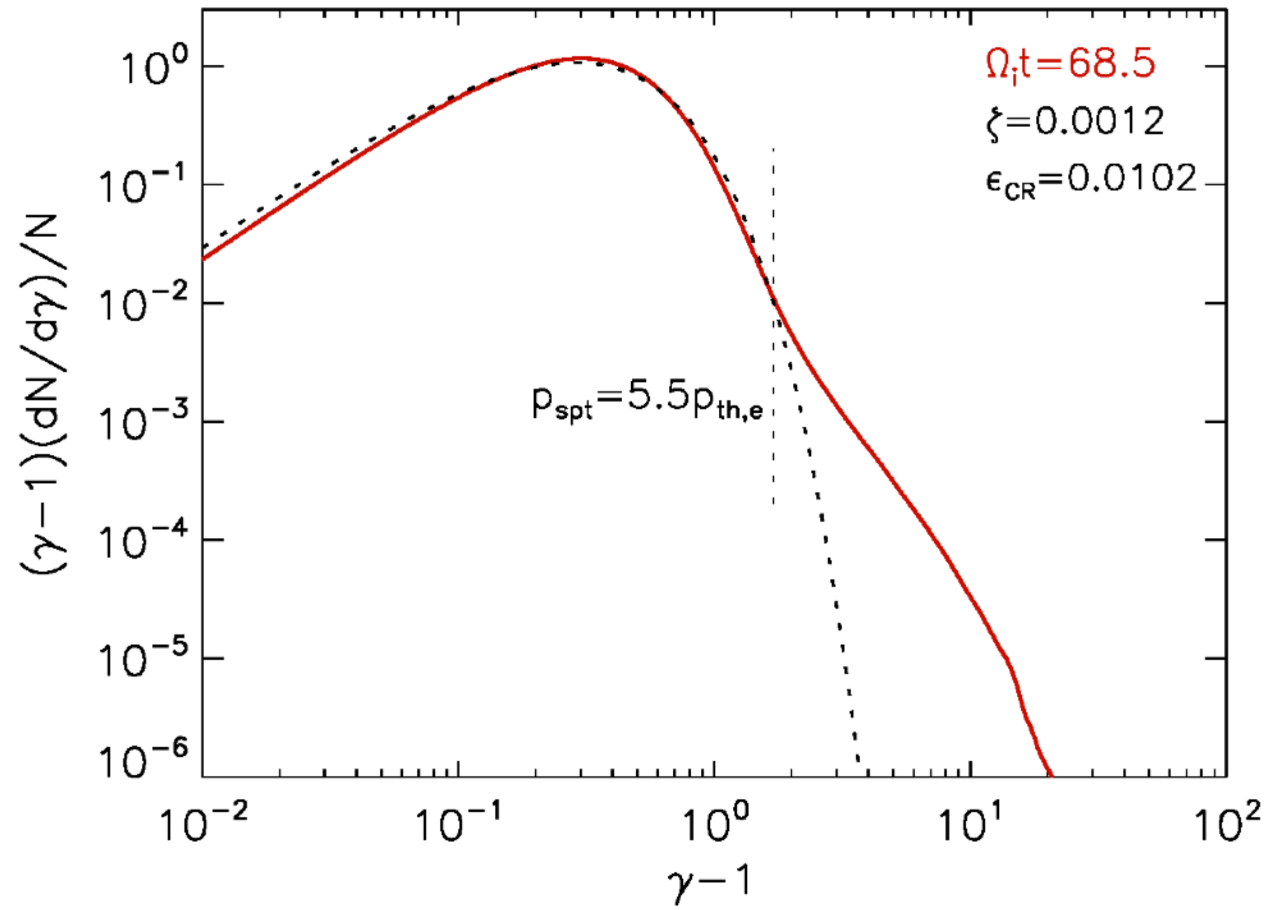

$$\zeta = \frac{4\pi}{N}\int_{p_{min}}^{p_{max}} \langle f(p)\rangle\, p^2 dp$$ - fraction of supra-thermal electrons

$\epsilon_{\rm CR}$ - corresponding energy density fraction

$\zeta_{\rm max,up} \simeq 5\%, \;\; \epsilon_{\rm CRmax,up} \simeq 40\%$

$\gamma_{\rm max,up} \approx 40 - 60 \quad \leftarrow \gamma_{\rm inj} \approx 25 \;\; (p_{\rm inj} \sim 3\, p_{\rm th,i})$

$\zeta_{\rm down} \simeq 0.12\%, \;\; \epsilon_{\rm CR,down} \simeq 1\%$

$\gamma_{\rm max,down} \simeq 20$

Acceleration processes - typical particle trajectories

- most particles gain their energies in a single interaction with the shock
- acceleration time much longer than predicted by SDA (~$1/\Omega_i$)
- highest-energy electrons produced at the shock front via interactions with long-wave ripples
- bulk of high-energy electrons accelerated deep in the shock transition

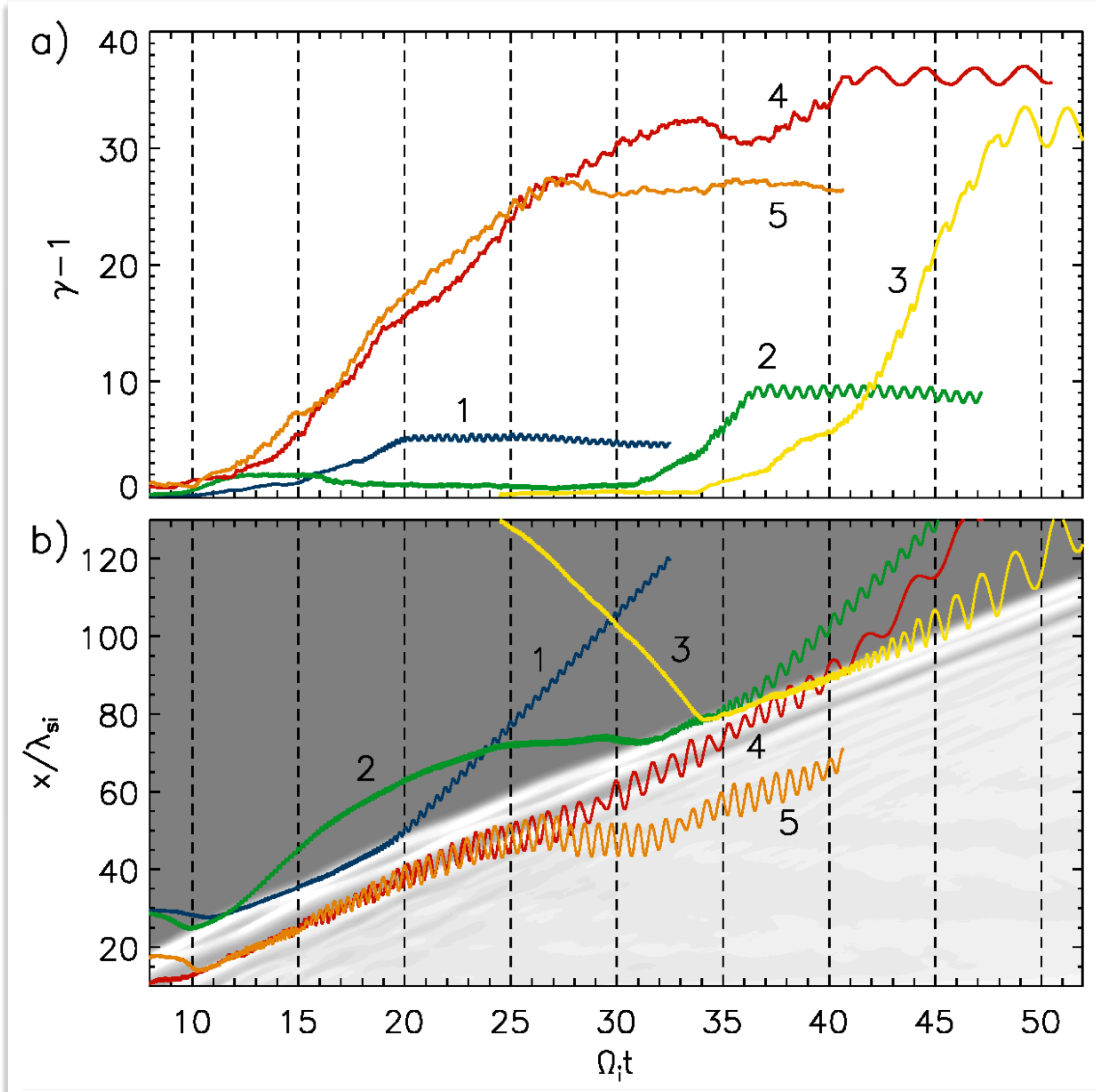

(β=5, ϑ_{Bn}=75°)

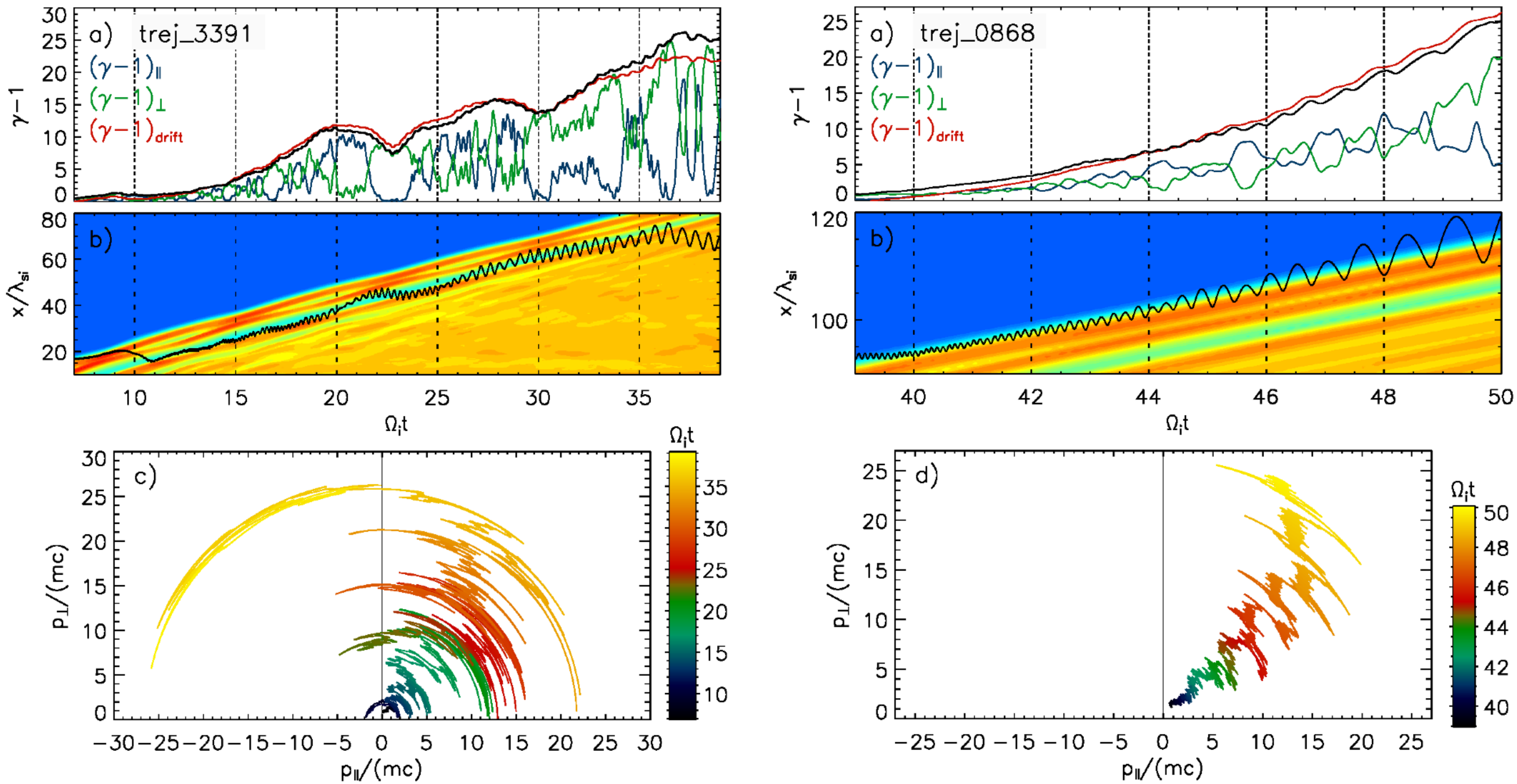

- most accelerations associated with an increase in $p_{\perp}$
- strong pitch-angle scattering (arcs in $p_{\parallel}$-$p_{\perp}$ momentum space)
- energy gain mostly through the drift along motional electric field:

$$\Delta\gamma_{\rm drift} = (-e/m_{\rm e}c^2)\int E_z\,dz$$

➜ Stochastic Shock-Drift Acceleration (SSDA)

Stochastic Shock Drift Acceleration (SSDA)

Katou & Amano (2019)

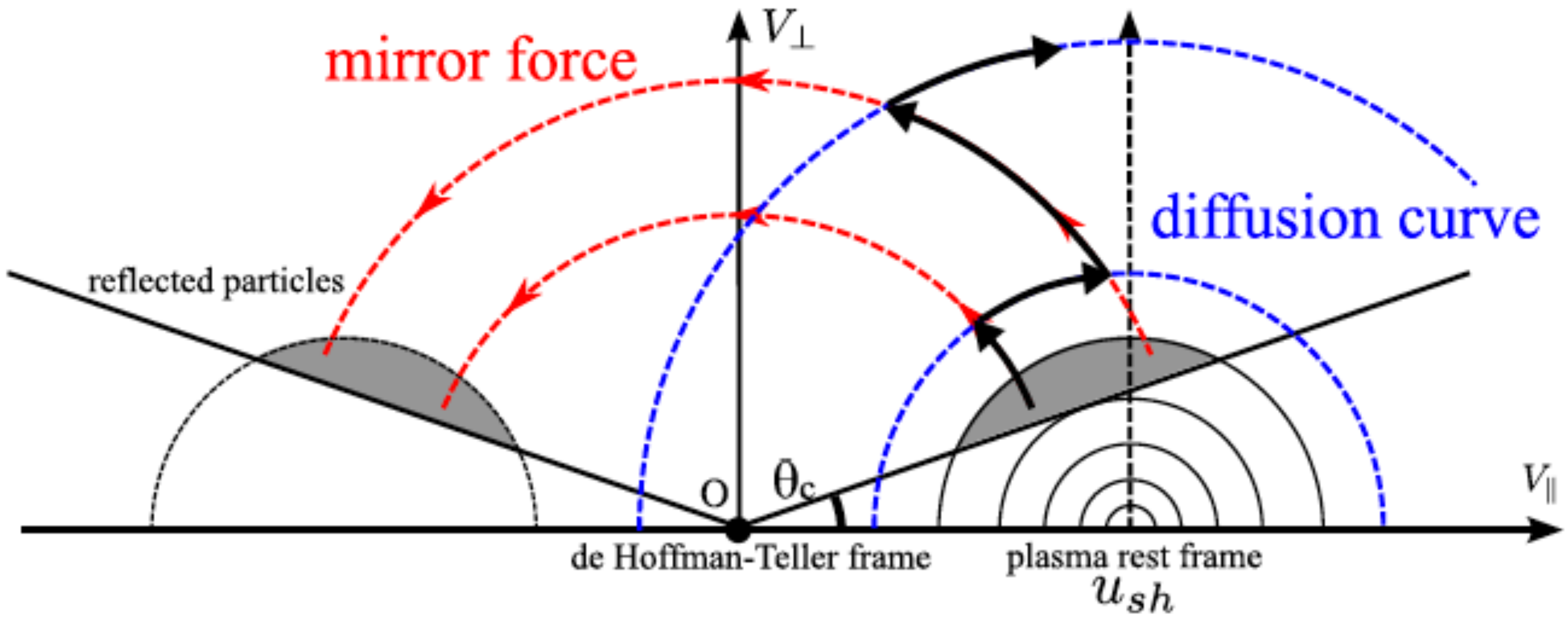

- adiabatic mirror reflection in the HTF
- elastic scattering (diffusion) in the plasma rest frame

- electrons are confined in the shock transition region by stochastic pitch-angle scattering off magnetic turbulence and gain energy through SDA (non-adiabatic acceleration)
- longer particle confinement increases energy gains and enables more efficient acceleration than standard SDA

- observational evidence for electron injection via SSDA at the Earth's bow shock recently provided by Magnetospheric Multiscale mission (Oka et al. 2017, Amano et al. 2020) - high-frequency whistlers

- SSDA observed in 3D PIC simulations of quasi-perpendicular high Mach number shocks of young supernova remnants (M_s=22.8, β=1; Matsumoto et al. 2017) - Weibel instability modes at the shock foot

- also observed in hybrid PIC and test-particle studies of solar wind shocks (M_s=6.6, β=1; Trotta & Burgess 2019) - shock-surface fluctuations

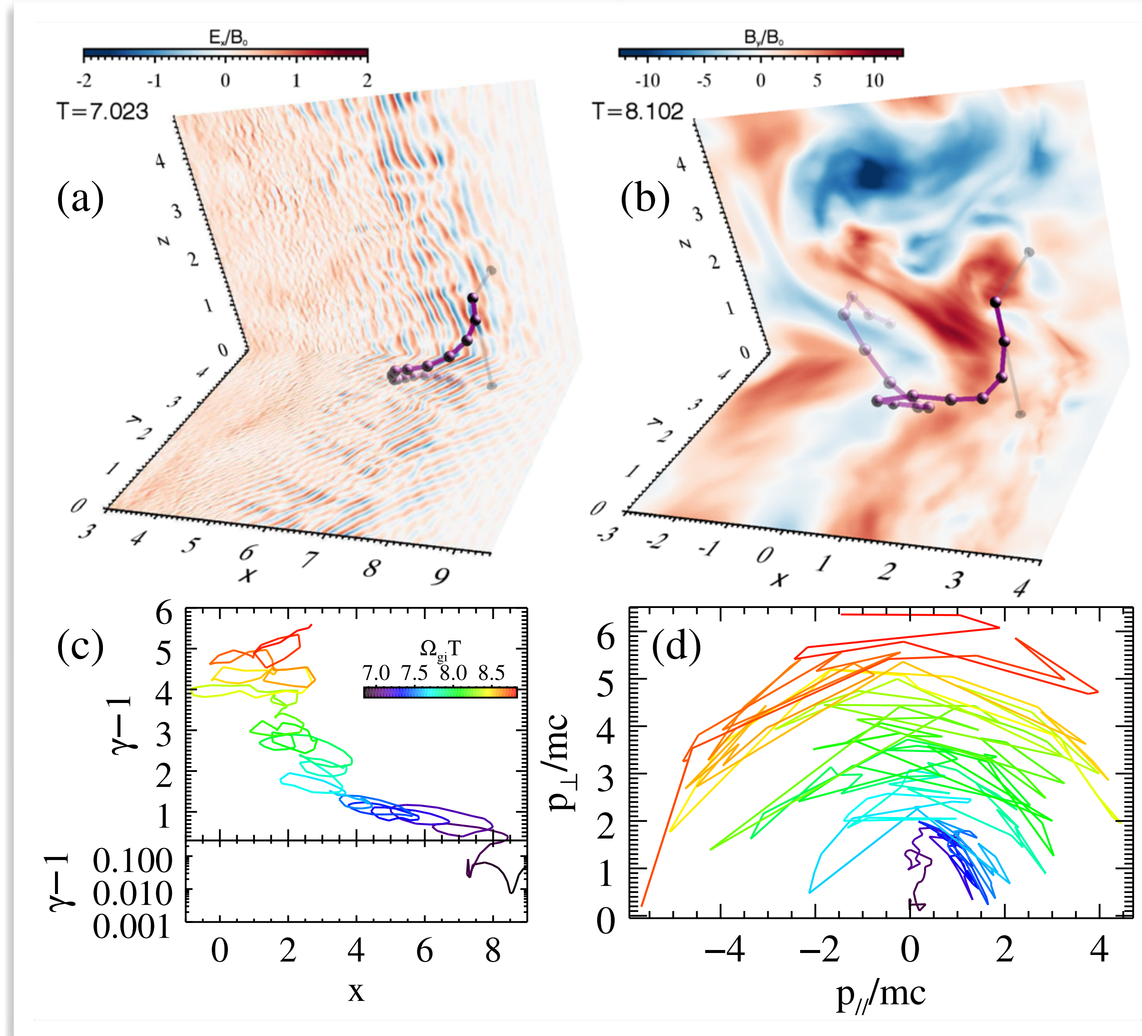

Matsumoto et al. (2017)

3D, M_A=20.8, M_s=22.8, ϑ=74.3°, m_i/m_e=64, β=1

- results for shocks with β=5 and ϑ_{Bn}=75° show that the electron scattering can be due to multi-scale (broad-band) turbulence in the entire shock transition

Parameter dependence - multi-scale turbulence

Kobzar et al. 2024 (2D PIC, in prep.)

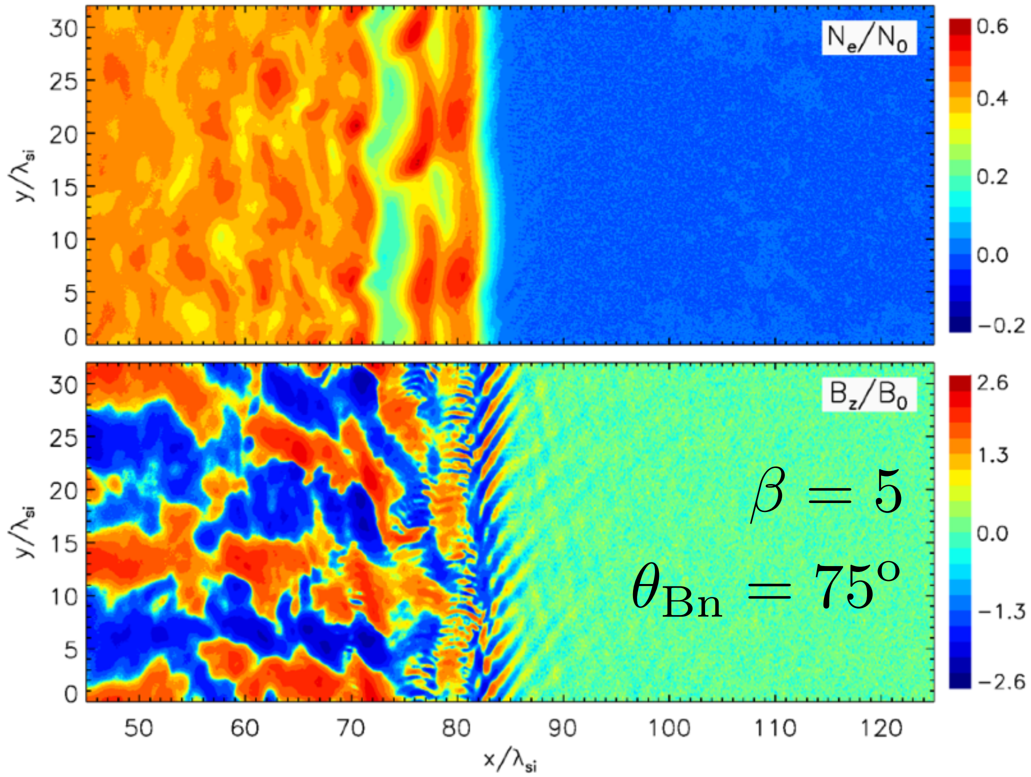

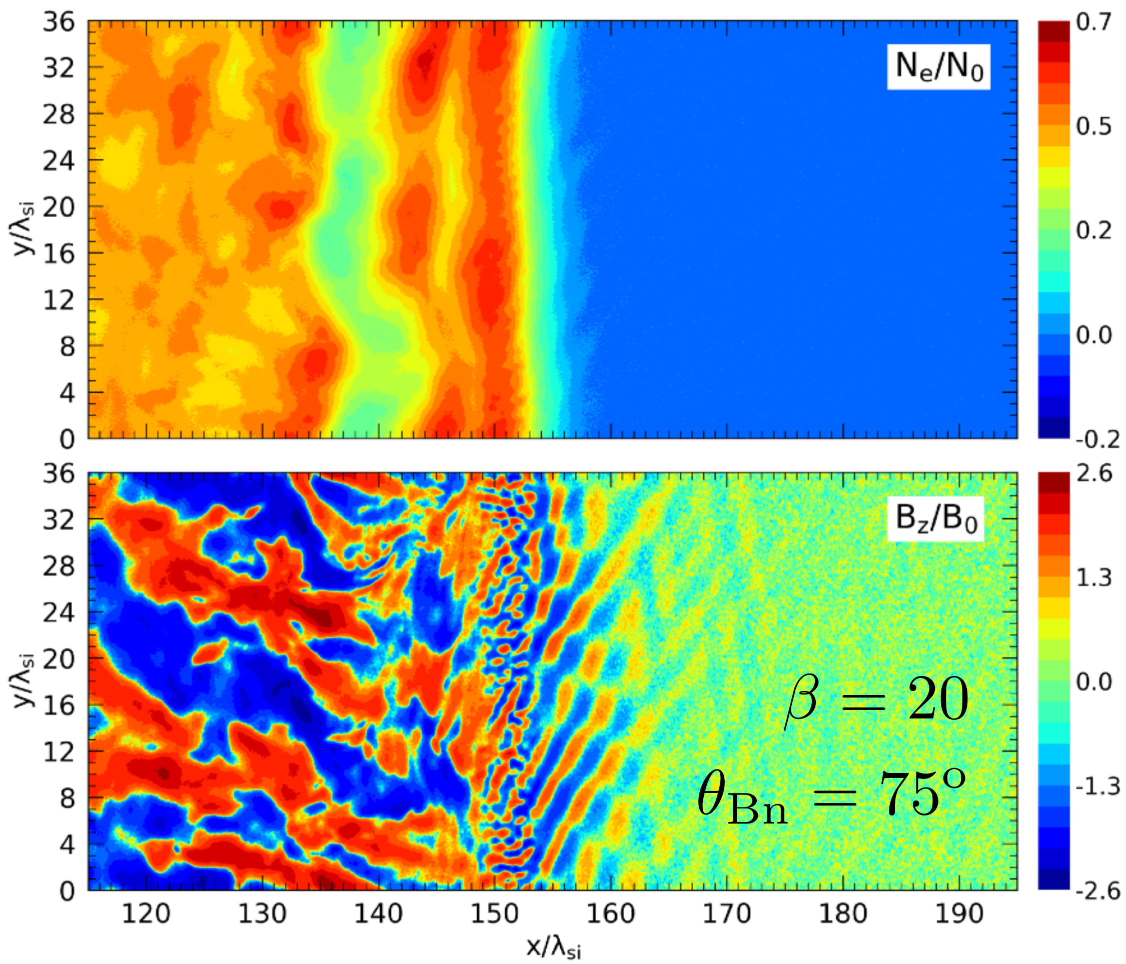

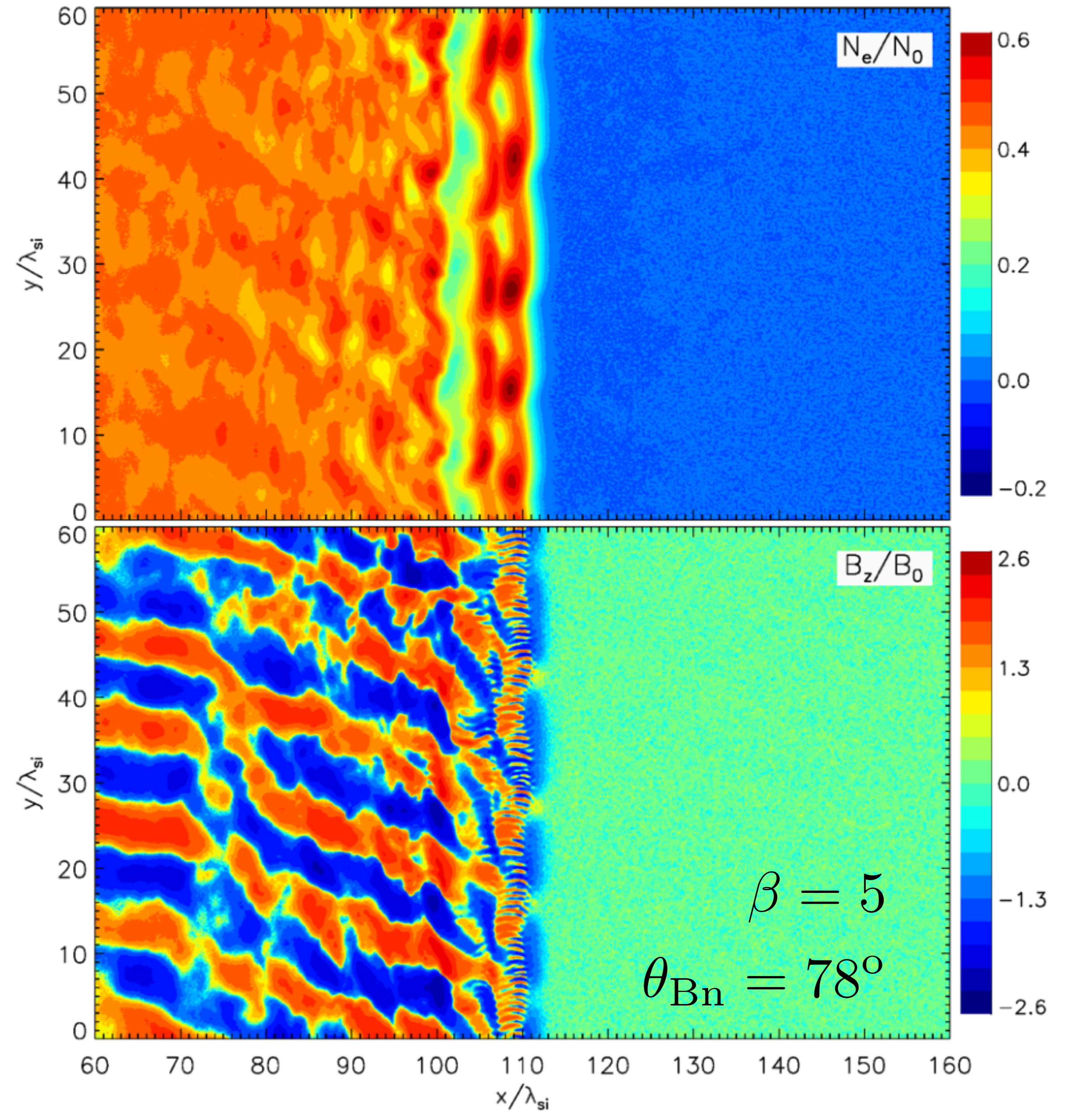

- features of multi-scale turbulence similar in all cases (M_s=3)
- longer-wavelength ripples with growing β
- absence of EFI waves for higher θ_{Bn}
- stronger and longer-wavelength EFI modes with increasing β (after amplification in rippled shocks)

Parameter dependence - upstream spectra

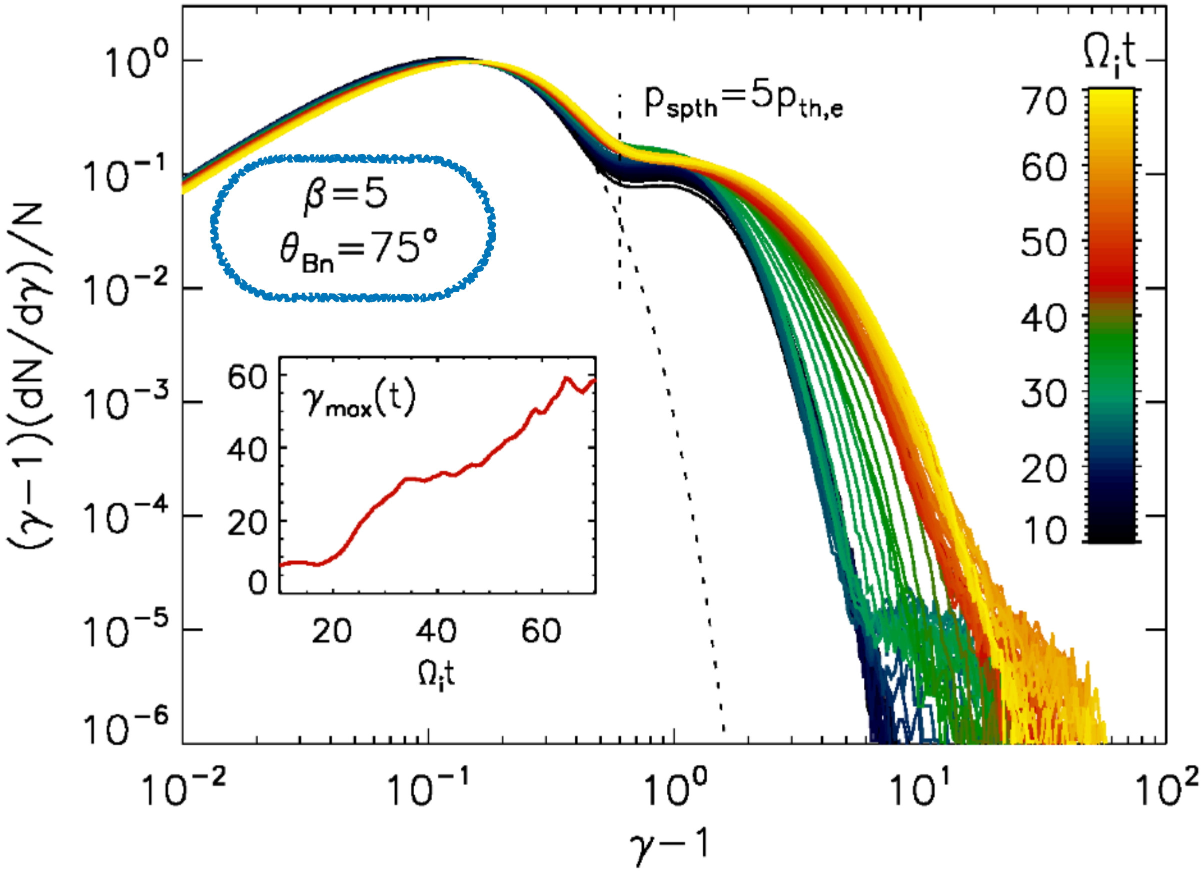

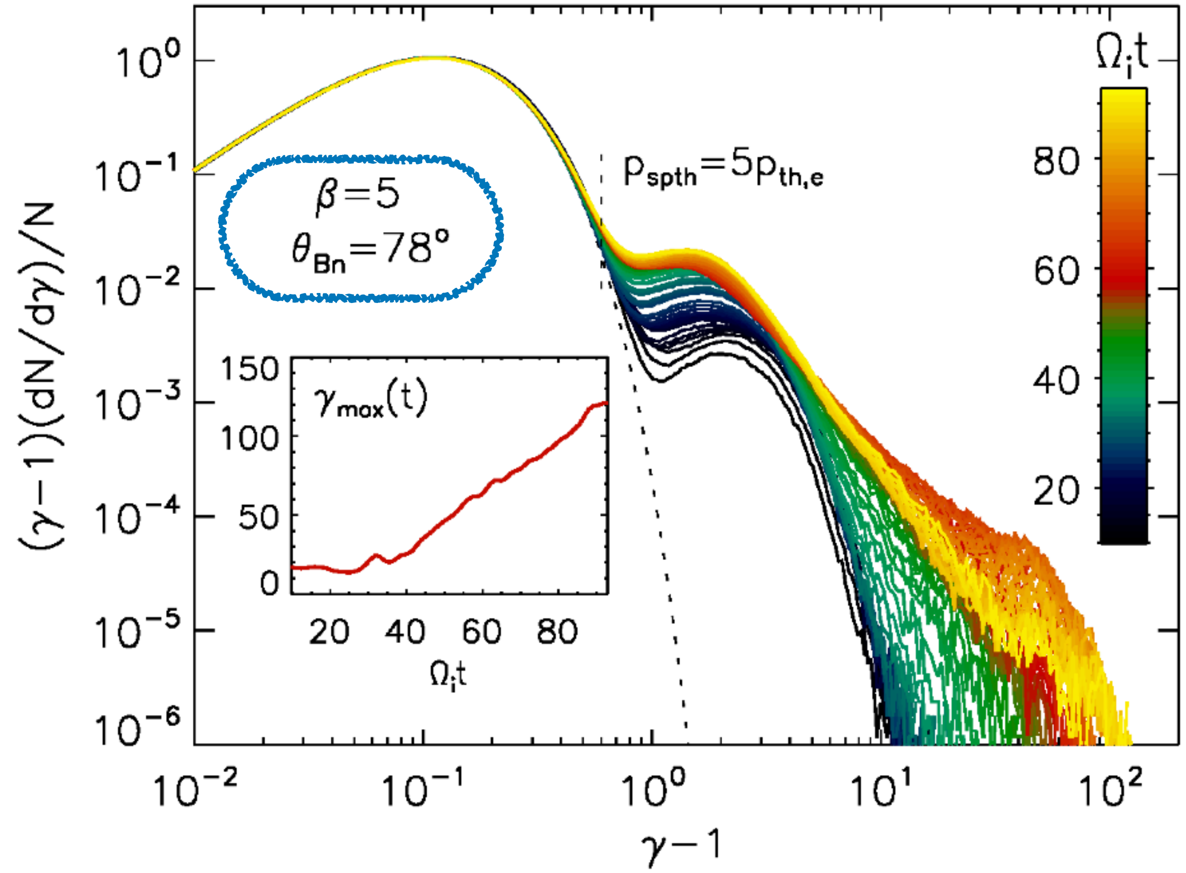

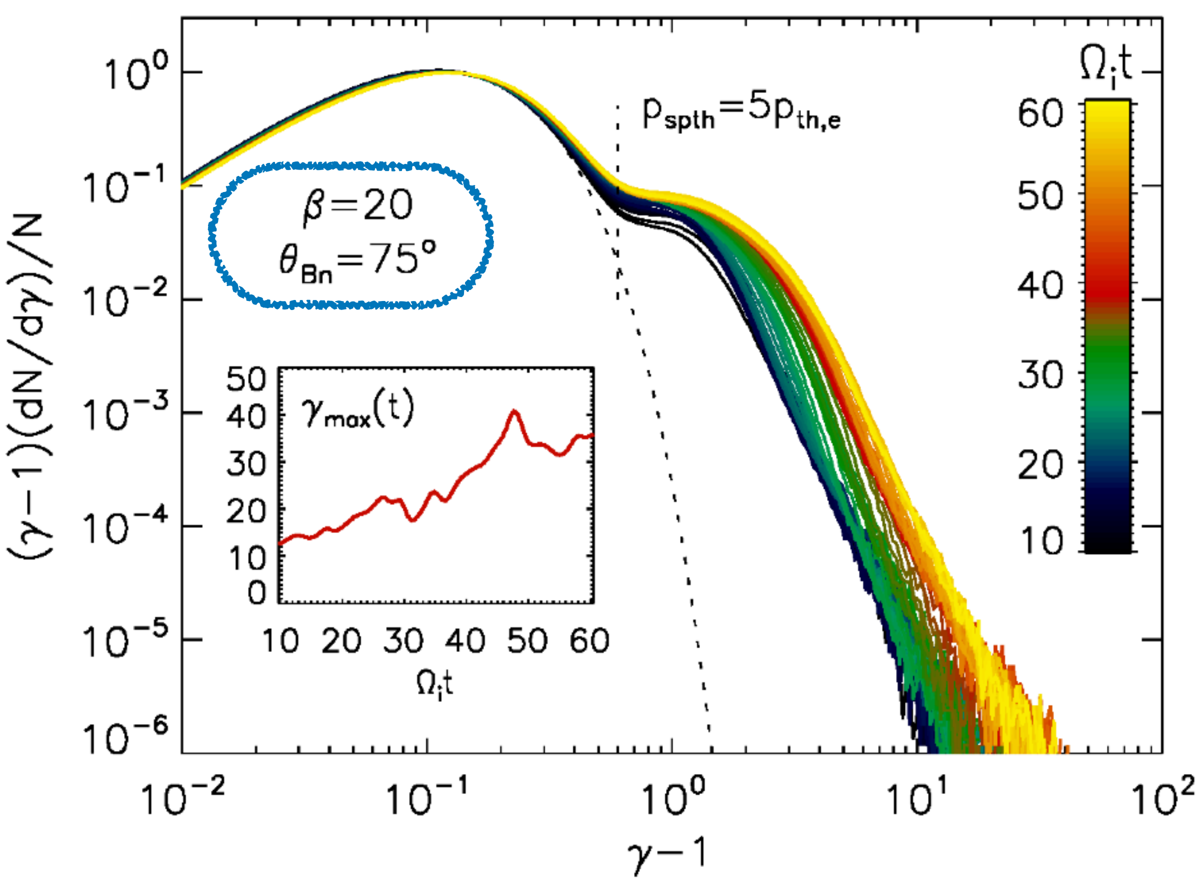

- SSDA in rippled shocks provides electron acceleration also for higher β=10-30 (checked up to β=100 - Ha et al. 2021)
- upstream spectra depend weakly on β
- maximum energies γ_{max}~30-120 > γ_{inj}
- multiple-cycle SDA is not critical for injection but may contribute to electron acceleration in high-β plasmas

Kobzar et al. 2024 (2D PIC, in prep.)

Implications for electron pre-acceleration from hybrid-PIC simulations; **open questions**

Boula et al. 2024

- 2D and 3D large-scale hybrid-kinetic simulations (kinetic ions, fluid electrons)
- simulations performed in a range of quasi-perpendicular foreshock conditions, including plasma beta, magnetic obliquity, and the shock Mach number
- studies of the ion kinetic physics, which is responsible for the shock structure and ion-scale wave turbulence, that in turn affects the particle acceleration processes; spatial and temporal scales larger than feasible with fully kinetic PIC simulations

Comparison with PIC simulations for ($\beta = 5$, $M_s = 3$, $\theta_{\mathrm{Bn}} = 75^{\mathrm{o}}$)

$t\Omega_{\mathrm{ci}} = 10$ (14)

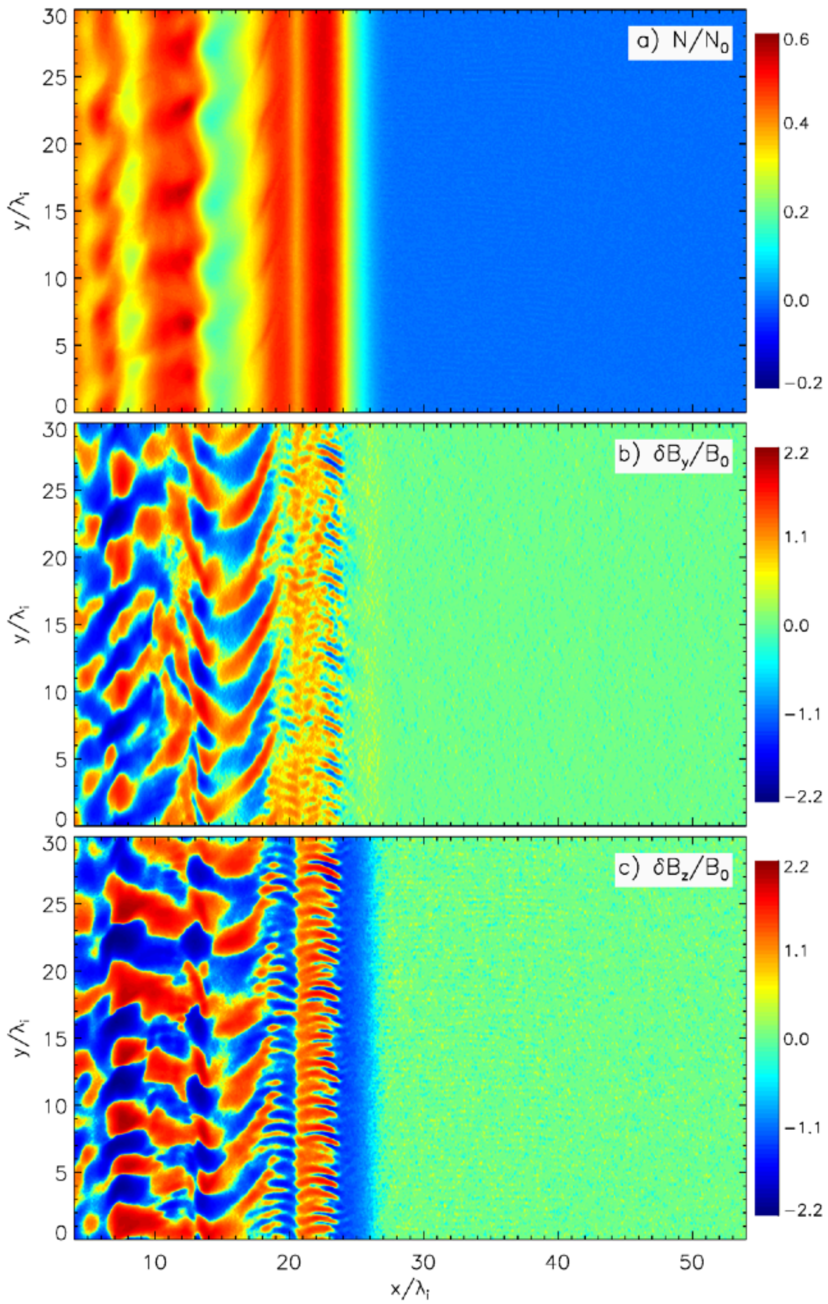

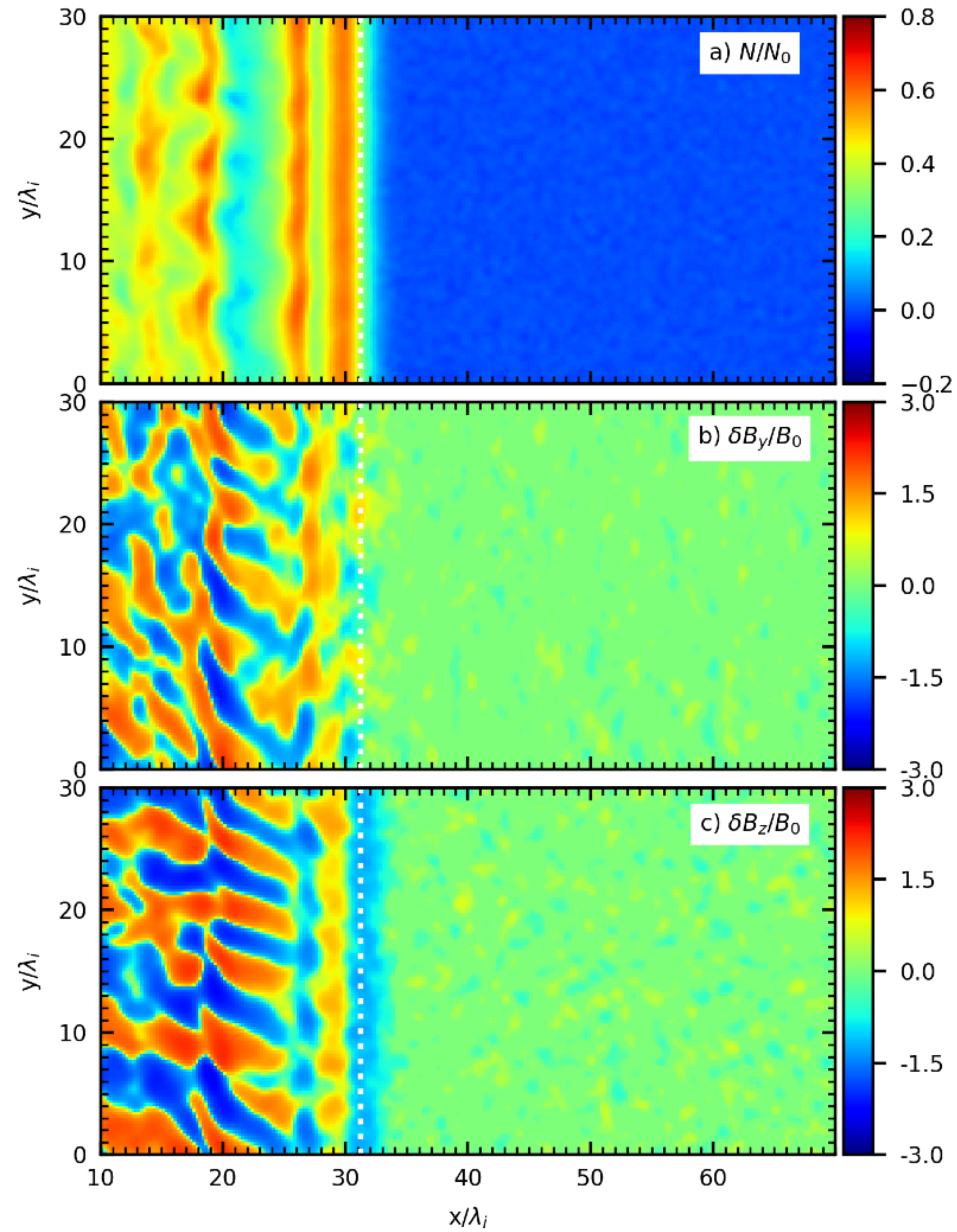

- in PIC simulations whistler waves strongest in the linear phase
- ion-scale fluctuations grow in parallel; their structure and evolution in good agreement with PIC simulations - **hybrid simulations reliable for ion-scale shock physics studies**

Implications for electron pre-acceleration from hybrid-PIC simulations; **open questions**

- Maximum energies in a range of shock conditions above γ_{inj} but transition to DSA not demonstrated self-consistently
- The growth of magnetic waves and shock corrugations saturates at λ_{ripple}~4 r_{gi}, which imposes constraints on the maximum energies of electrons confined at the shock through scattering - is this enough for injection?

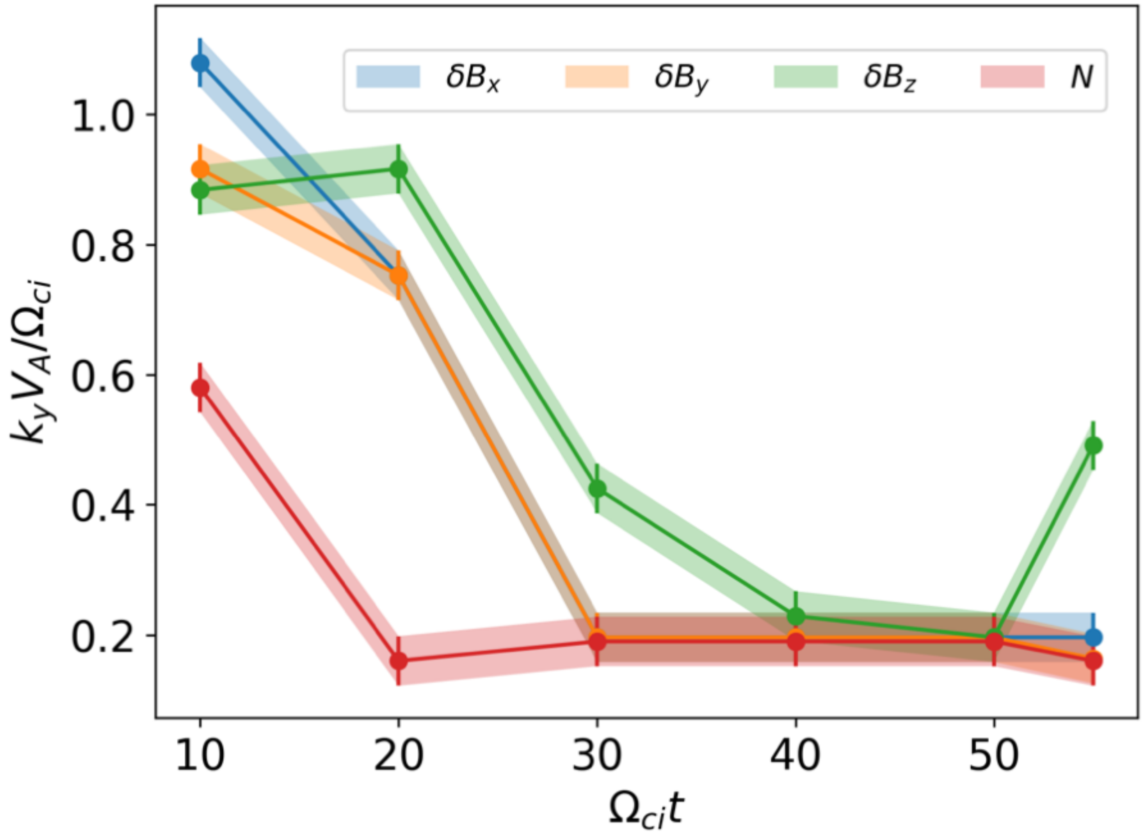

Boula et al. 2024 (2D hybrid); β=20

Implications for electron pre-acceleration from hybrid-PIC simulations; **open questions**

- SSDA demonstrated to work at M_s=3 shocks
- some radio relics have M_s~1.5-2.3; how electrons are injected at such shocks?

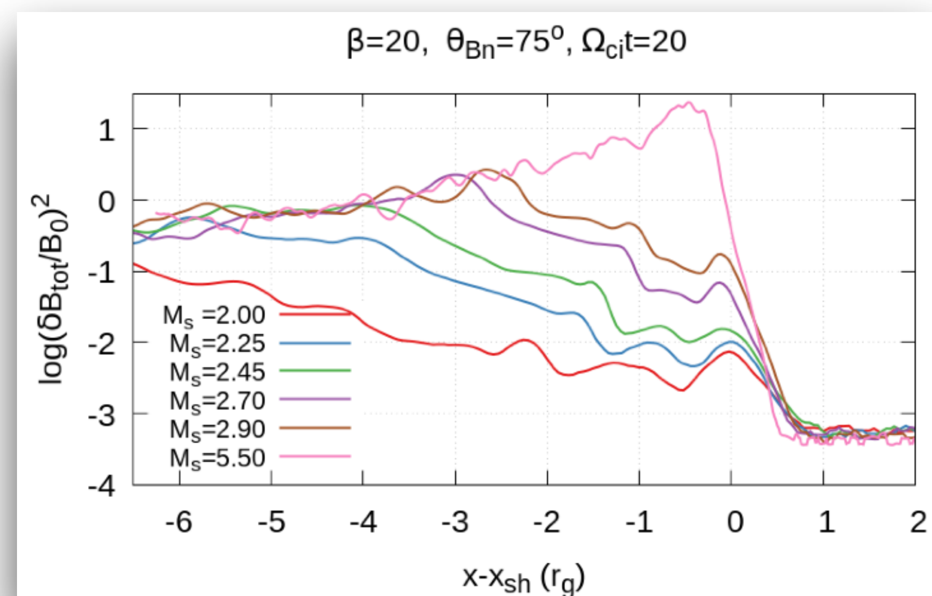

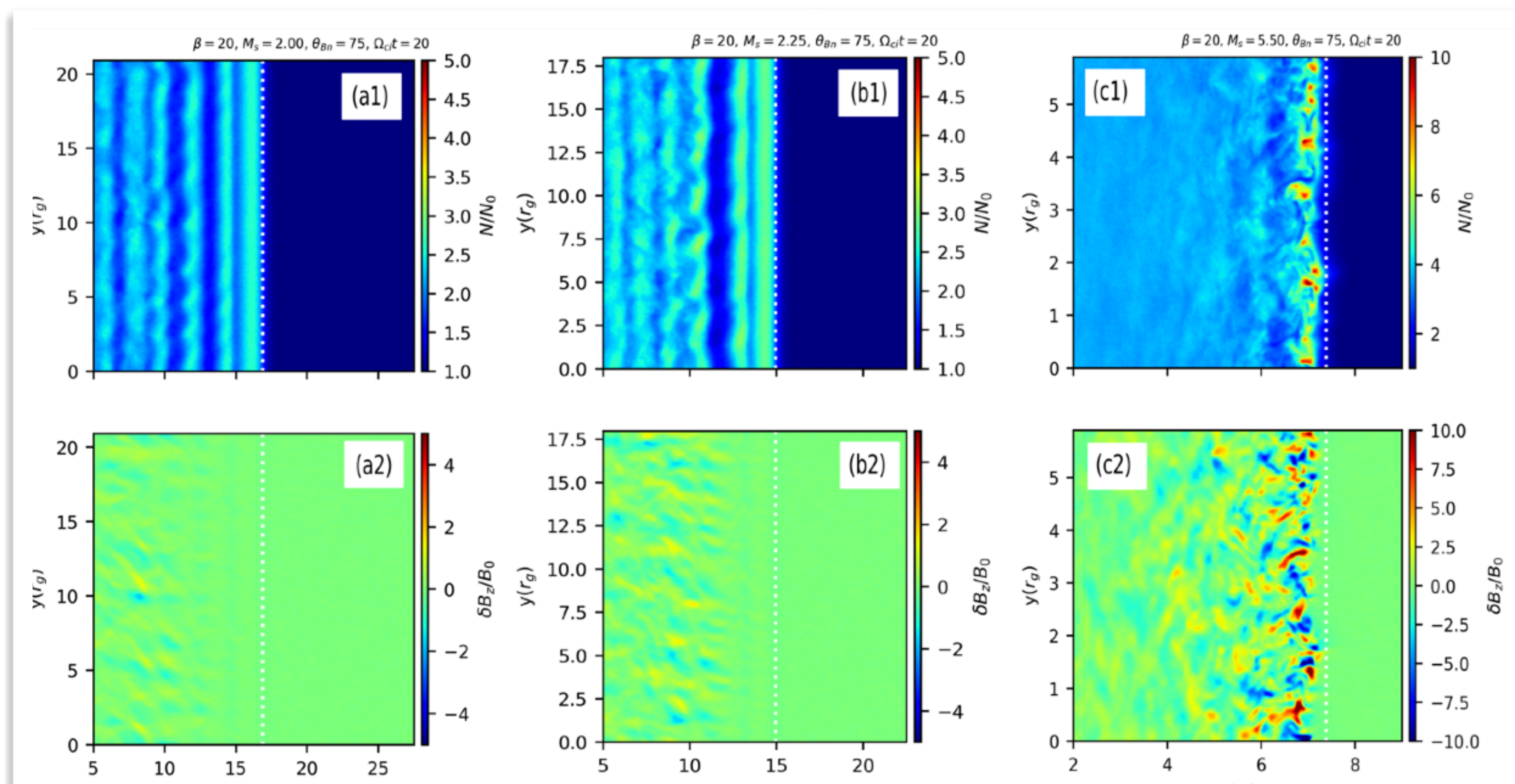

M_s=2.0 M_s=2.25 M_s=5.5

Boula et al. 2024 (2D hybrid); β=20

- what is shock physics in 3D?
- there is little difference between 2D and 3D simulations. Turbulence near the shock front seems to be a 2D-like structure in 3D simulations.

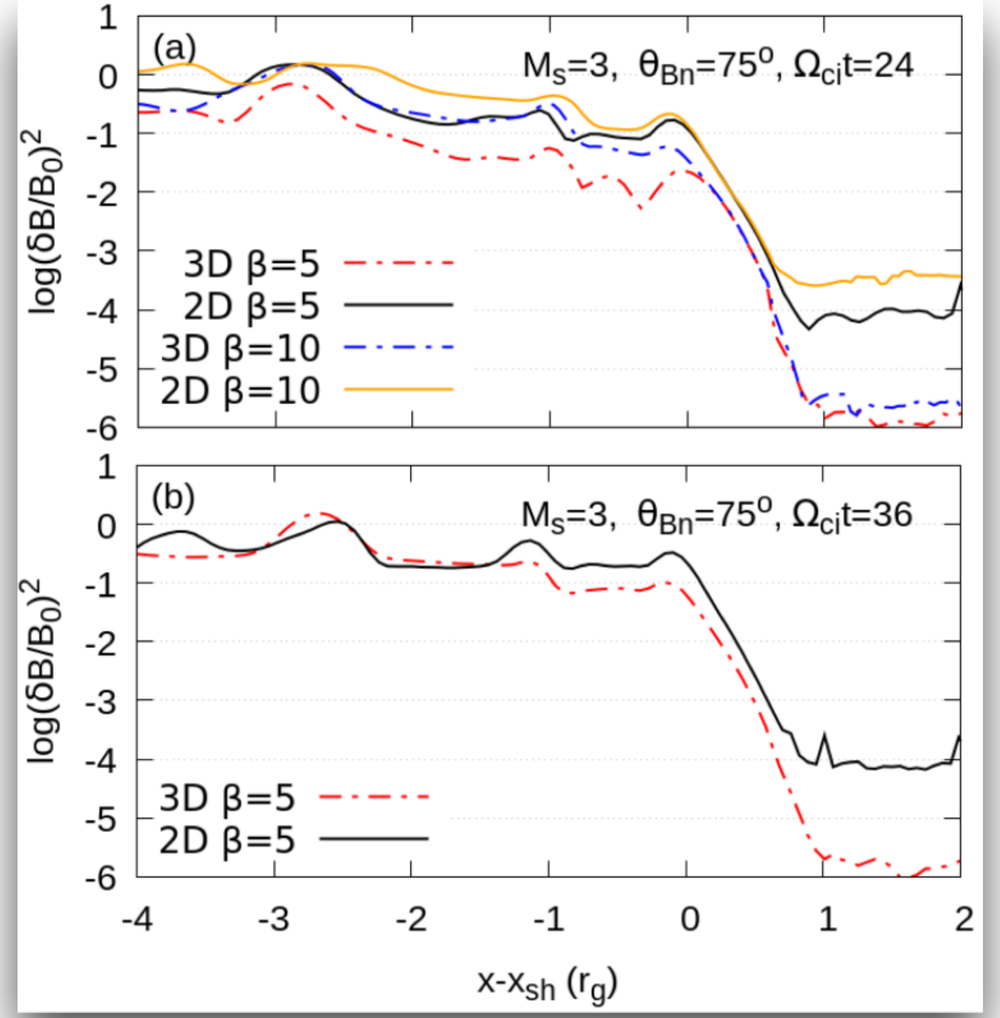

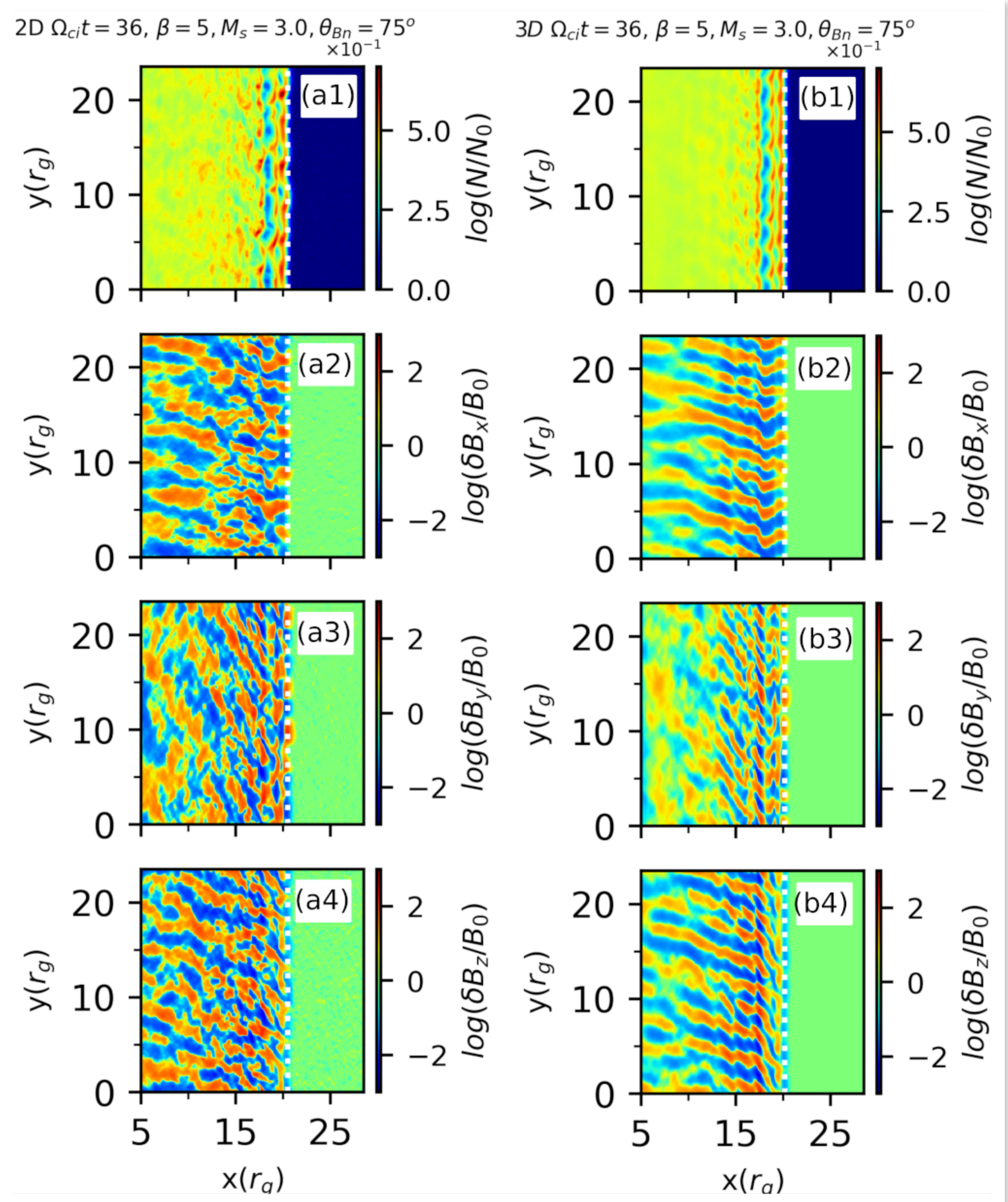

Boula et al. 2024 (2D hybrid); β=5, 10

Summary and conclusions

- modeling of particle acceleration at low Mach number shocks in high-beta plasmas requires multi-dimensional and large-scale effects to be taken into account
- the presence of multi-scale turbulence, including ion-scale shock rippling modes, is critical for efficient electron acceleration that proceeds mainly through the stochastic SDA process
- electrons can be injected to DSA at supercritical quasi-perpendicular sub-luminal ICM shocks that develop multi-scale turbulence
- pre-acceleration to high energies is feasible, at which DSA starts to operate in the presence of long-wave (MHD) upstream turbulence
- electron injection at lower Mach number shocks requires further studies

This work has been supported by Narodowe Centrum Nauki through research project 2019/33/B/ST9/02569.
We gratefully acknowledge Poland's high-performance Infrastructure PLGrid HPC Center ACK Cyfronet AGH for providing computer facilities and support within computational grant no. PLG/2023/016861.